OXFORD UNIVERSITY PRESS | Tree Physiology

Variation in the access to deep soil water pools explains tree-to-tree differences in drought-triggered dieback of Mediterranean oaks

Journal:	*Tree Physiology*
Manuscript ID	TP-2019-503.R1
Manuscript Type:	Research Paper
Date Submitted by the Author:	n/a
Complete List of Authors:	Ripullone, Francesco; University of Basilicata, School of Agricultural, Forest, Food and Environmental Sciences Camarero, Jesús; Instituto Pirenaico de Ecología (CSIC), Departamento de Conservación de Ecosistemas Naturales Colangelo, Michele; University of Basilicata, School of Agricultural, Forest, Food and Environmental Sciences Voltas, Jordi; University of Lleida, Crop Production and Forest Science
Keywords:	deuterium, Drought Stress, Dendrochronology, Quercus, Tree Growth

Variation in the access to deep soil water pools explains tree-to-tree differences in drought-triggered dieback of Mediterranean oaks

Francesco Ripullone[1]*, J. Julio Camarero[2], Michele Colangelo[1,2], Jordi Voltas[3,4]

[1]School of Agricultural, Forest, Food and Environmental Sciences, Univ. Basilicata, Potenza I-85100, Italy. E-mails: francesco.ripullone@unibas.it; michelecolangelo3@gmail.com

[2]Instituto Pirenaico de Ecología (IPE-CSIC), Avda. Montañana 1005, Zaragoza E-50059, Spain. E-mail: jjcamarero@ipe.csic.es

[3]Joint Research Unit CTFC - AGROTECNIO, Av. Alcalde Rovira Roure 191, 25198 Lleida, Spain.

[4]Department of Crop and Forest Sciences, Universitat de Lleida, Av. Alcalde Rovira Roure 191, 25198 Lleida, Spain. E-mail: jvoltas@pvcf.udl.cat

*Corresponding author:

Francesco Ripullone
[1]School of Agricultural, Forest,
Food and Environmental Sciences
University of Basilicata
Potenza, 85100 Italy
E-mail: francesco.ripullone@unibas.it

Key words: die-off, drought stress, Quercus, soil water sources, water isotopes.

Summary

Individual differences in the access to deep soil water pools may explain the differential damage among coexisting, conspecific trees as a consequence of drought-induced dieback. We addressed this issue by comparing the responses to a severe drought of three Mediterranean oak species with different drought tolerance: *Quercus pubescens* and *Quercus frainetto*, mainly thriving at xeric and mesic sites respectively, and *Quercus cerris*, which dominates at intermediate sites. For each species we compared coexisting declining (D) and non-declining (ND) trees. The stable isotope composition (δ^2H, $\delta^{18}O$) of xylem and soil water was used to infer a differential use of soil water sources. We also measured tree size and radial growth to quantify the long-term divergence of wood production between D and ND trees, and non-structural carbohydrates (NSC) in sapwood to evaluate if D trees presented lower NSC values. ND trees had access to deeper soil water than D trees except in *Q. frainetto*, as indicated by significantly more depleted xylem water values. However, a strong δ^2H offset between soil and xylem water isotopes observed in peak summer could suggest that both tree types were not physiologically active under extreme drought conditions. Alternative processes causing deuterium fractionation, however, could not be ruled out. Tree height and recent (last 15-25 years) growth rates in all species studied were lower in D than in ND trees by 22% and 44%, respectively. Lastly, there was not a consistent pattern on NSC sapwood concentration, showing that in *Q. pubescens* was higher in ND trees, while in *Q. frainetto* the D trees were the ones exhibiting the higher NSC concentration. We conclude that the vulnerability to drought among conspecific Mediterranean oaks depends on the differential access to deep soil water pools, which may be related to differences in rooting depth, tree size and growth rate.

Introduction

Drought-induced dieback is a global phenomenon affecting all forest biomes (Allen et al. 2015). However, neither all tree species in a community nor all tree individuals in a population are similarly affected by drought. Several studies have evidenced a diverse vulnerability to drought damage among coexisting individuals of different or the same species as a function of site features (dryness, drought intensity) or tree structural (e.g. height), hydraulic (e.g. conduit size, loss of hydraulic conductivity, hydraulic conductance) and functional characteristics (e.g., deciduousness, leaf size and density, sapwood density, root depth, gas exchange rates) (Adams et al. 2017, Greenwood et al. 2017, Martin-StPaul et al. 2017, Choat et al. 2018, Johnson et al. 2018, Olson et al. 2018, Liu et al. 2019). These studies have attempted to link such features to the major mechanisms underlying forest dieback, namely hydraulic failure and carbon starvation (McDowell et al. 2008).

Measures of drought damage such as growth decline, leaf shedding, canopy dieback or high mortality rates have been associated to traits as xylem vulnerability to cavitation or low wood density (Nardini et al. 2013). Tree species with dense wood and low specific leaf area tend to show lower post-drought mortality rates than species with the reverse characteristics (Greenwood et al. 2017). Hydraulic traits account for part of the variability in drought vulnerability across tree species, despite their potentially different importance for angiosperms and gymnosperms (Anderegg et al. 2016). For instance, tall gymnosperms are forecasted to be more prone to die due to water shortage than short-stature, hydraulically more efficient angiosperms (McDowell and Allen 2015). A similar reasoning has been applied at the community level in a way that the

diversity in species hydraulic traits in temperate and boreal forests explained part of the ecosystem carbon fluxes after a drought (Anderegg et al. 2018). Yet within a particular forest, predicting which tree species and individuals are most likely to die or survive after a severe drought remains a challenge. Individual tree predispositions due to either differential plastic responses or constitutive genetic differences for functional traits related to drought resistance could buffer damage due to drought stress (Voltas et al. 2013).

At stand level, variability in traits related to drought resistance is expected to show a wider range between than within species. Therefore, understanding and quantifying the vulnerability to drought within a species is a first step towards predicting the probability of individual survival. Growth trends (tree-ring-width data) have been related to crown dieback and used as early-warning signals to identify and characterize declining and, therefore, more vulnerable individuals within a species (Camarero et al. 2015). However, this approach seems feasible in some species, for instance in some conifers whose susceptible individuals show long periods (>20 yrs.) of growth decline, but not in others as oaks which show shorter periods (5-20 yrs.) of growth reduction (Cailleret et al. 2018). This may be due to the fact that oaks display an anisohydric behavior with pronounced declines in leaf midday water potential during drought and may be prone to xylem cavitation and hydraulic failure, whereas isohydric conifers rapidly close stomata as vapor pressure deficit (VPD) rises (Klein 2014). In the case of ring-porous Mediterranean oak species, hotter droughts may enhance atmospheric evaporative demand shifting VPD towards a critical threshold, surpassing their limit of hydraulic safety (Tognetti et al. 1998, Colangelo et al. 2017a). Consequently, hydraulic failure could be a plausible mechanism of drought-induced dieback in Mediterranean oaks.

Drought-tolerance mechanisms are diverse and not restricted to resistance to xylem cavitation, stomatal control of water use or increased carbon storage (Pinheiro et al. 2005). These mechanisms also include different access to soil water pools, with shallow- and deep-rooted species often showing high and low drought damage levels, respectively (Padilla and Puignaire 2007, Hasselquist et al. 2010, Pivovaroff et al. 2016, Antunes et al. 2018, Chitra-Tarak et al. 2018). Drought stress often acts as a major driver of dieback, usually linked to site-specific soil conditions, such as the characteristics of soil parent material that inhibits root development or access to groundwater (Costa et al. 2010). Indeed, large belowground losses of hydraulic conductance and shallow rooting depths are often associated with species that exhibit greater mortality after severe droughts (Johnson et al. 2018). According to stable isotope evidence, roots may take up deep soil water during dry periods which allow trees to buffer drought effects (Ehleringer and Dawson1992, Barbeta and Peñuelas, 2017). Coexisting species may show different water isotopic signals corresponding to contrasting – and highly dynamic – water-use strategies during drought as observed in Mediterranean forests (Moreno-Gutierrez et al. 2012, Del Castillo et al. 2016, Dubbert et al. 2019, Dubbert and Werner 2019). However, tree species may tap increasingly deep sources of soil water as drought intensifies (Meinzer et al. 1999, Voltas et al. 2015). The access to deep water reservoirs could buffer the predicted negative impacts of hotter droughts on forests (Sánchez-Salguero et al. 2017) and allow trees to survive and recover in hydrologic refugia where groundwater is available throughout the year (McLaughlin et al. 2017).

Here we test the idea that tree-to-tree differences in the use of deep soil water may explain the differential damage of coexisting, conspecific oak individuals due to drought-induced dieback. For this purpose, we use information of the stable isotope

composition ($\delta^{18}O$ and $\delta^{2}H$) of soil and xylem water obtained at the peak of summer drought. We also quantify changes in radial growth and in the sapwood concentration of non-structural carbohydrates (NSC) of conspecific trees showing different vulnerability to drought. We expect that non-declining, asymptomatic trees will be able to extract water from deeper soil water pools than declining, symptomatic trees. We also expect this difference to be magnified in the species occupying the most xeric sites (*Q. pubescens*), subjected to frequent and intense episodes of water shortage, compared with the species typical of mesic sites (*Q. frainetto*), which grows more, depends on shallower soil water and has a lower root-to-shoot ratio (Ledo et al. 2018). Lastly, we hypothesize that declining trees will show a lower sapwood NSC concentration than non-declining trees.

Materials and methods

Study sites

We studied three Mediterranean, deciduous, ring-porous oak species in southern Italy: two species (*Quercus pubescens* L., *Quercus cerris* L.) were sampled in different stands located at the Gorgoglione municipality (40° 21’ 51’’ N, 16° 10’ 34’’E, 825 m a.s.l.), and the third species (*Quercus frainetto* Ten.) was sampled in a stand near San Paolo Albanese (40° 01’ 20’’ N, 16° 20’ 46’’ E, 950 m a.s.l.). *Q. pubescens* is widely distributed across southern Europe, *Q. cerris* is found in the Italian and Balkan Peninsulas, Asia Minor, central Europe and France, and *Q. frainetto* is found across the Western Mediterranean Basin (San-Miguel-Ayanz et al. 2016). These species often coexist (and hybridize) in sites with mean annual temperature (MAT) of 6-18 ºC and annual precipitation (MAP) of 500-1300 mm. In the study areas climate is Mediterranean, characterised by dry and warm summers that have become particularly

noticeable during the last decade (Fig. 1). At San Paolo Albanese, total June to August precipitation is 79 mm and winters are wet and mild. At this site, MAT is 16.4 °C and MAP is 742 mm (data from Oriolo station, 40° 03'11''N, 16° 26' 47'' E, 445 m a.s.l., 1950–2016 period). At Gorgoglione, total June to August precipitation is 93 mm and winters are wet and mild. At this site, MAT is 14.6 °C and MAP is 722 mm (data from Gorgoglione station, 40' 240'' N, 16' 090'' E, 796 m, 1950–2016 period). In both sites drought occurs from June to August.

To assess long-term climate trends we used the E-OBS 0.25º-gridded climate dataset considering the 1950-2017 period (Cornes et al. 2018). We downloaded annual and monthly temperature and precipitation data for the grid with coordinates 16.00-16.25º W and 40.00-40.25º N using the climate explorer webpage (https://climexp.knmi.nl). We also estimated drought severity using the self-calibrating Palmer Drought Severity Index (hereafter PDSI) based on the gridded monthly precipitation and temperature data (Wells et al. 2004). We calculated the summer PDSI (from June to August) to quantify summer drought severity.

Soils are sandy-loam textured with a mean pH of 7.5 and mostly shallow (i.e. ranging from 0.2 to 0.6 m depth). They rest on a soft sedimentary fractured bedrock consisting of an alternation of sandstones, pelites and conglomerates layers (Gorgoglione Flysch Formation), which typify part of the Apennines chain.

In the study area, the three species coexist but *Q. pubescens* preferentially occupies the most xeric sites (e.g., steep slopes with southern aspect and shallow soils), *Q. frainetto* is found in mesic sites (e.g., gentle slopes with northern aspect and relatively deep soils), and *Q. cerris* abounds in intermediate locations (Gentilesca et al. 2017). In San Paolo Albanese, the vegetation is formed by a pure high forest of *Q. frainetto* for a density of 348 trees ha^{-1}, whilst in Gorgoglione the stand is a mixed high

forest with a mean density of 600 trees ha^{-1} dominated by *Quercus cerris* L. (71%), followed by *Quercus pubescens* L. (25%) and other broadleaf species (4%). These oak forests were formerly managed as coppices with livestock grazing.

All species have shown symptoms corresponding to drought-induced dieback since the turn of this century, specifically canopy dieback, leaf loss and withering, growth decline, and high mortality (Colangelo et al. 2017a, 2017b). In the most affected stands, more than 50% of mature specimens showed dieback symptoms and 15% recently died (Colangelo et al. 2018).

Field sampling

To characterize stand structure (density, basal area) and assess the degree of dieback damage we followed a similar procedure as in Colangelo et al. (2017a). Seven circular plots (radius of 15 m) were randomly located in each site and in areas where each species was dominant. Within each plot, dieback of all mature oak trees was characterized by a visual assessment of crown transparency made by two independent observations of the same tree (Camarero et al. 2016). Declining oaks (hereafter D trees) were considered those with crown transparency higher than 50%, whereas non-declining oaks (hereafter ND trees) were considered those with transparency lower than 50%. The size (diameter at 1.3 m, total height) of all trees was measured.

Radial growth

For each species, we selected 12-21 paired trees of different vigour, i.e. neighbouring ND and D oaks located 10–15 m apart at maximum. They were sampled in late summer of 2016 to quantify their radial-growth trends using dendrochronology. Two cores were

sampled at breast height (1.30 m) from each tree at opposite directions and perpendicular to the maximum slope using a 5-mm Pressler increment borer.

The transversal surface of cores was cut using a sledge microtome to differentiate the annual tree rings (Gärtner and Nievergelt 2010). Rings were visually cross-dated and measured with precision of 0.01 mm using a binocular microscope coupled to a computer with the LINTAB package (Rinntech, Heidelberg, Germany). The COFECHA program (Holmes 1983) was used to evaluate the visual cross-dating of tree-ring width data. To quantify growth trends and to partially avoid the age- / size-related decrease in tree-ring width, we transformed these data into annual basal area increment (BAI) assuming a circular shape of stems. Tree age at 1.3 m was estimated from increment cores that either included the pith or were close to it (the arc of the innermost rings was visible). In the second case, we followed Duncan (1989) and fitted a template of concentric circles to the curve of the innermost rings to estimate the number of missing rings.

Soil and xylem water sampling and extraction, groundwater collection and isotopic analyses

The soil and stem xylem sampling took place in August 2017 during an exceptionally hot and dry period, with a monthly temperature over 2 ºC higher and precipitation about 40 mm lower than long-term averages for the region (22.8 °C and 56 mm). This resulted in the most severe drought occurring over the last 70 years (Fig. 1). Information on the use of soil water sources for each species and tree type (D, ND) was obtained using measurements of water isotope ratios (oxygen and hydrogen isotope composition, $\delta^{18}O$ and $\delta^{2}H$) for different soil depths as well as for xylem water (Martín-Gómez et al. 2015, Grossiord et al. 2017).

Xylem samples were obtained from 11:00 to 13:00 h solar time from twelve D and twelve ND trees per species at Gorgoglione (August 23rd) and San Paolo Albanese (August 24th). Two branches were sampled from the upper third crown of each tree at north- and south-facing sides using telescopic loppers. Sampled branches were *ca*. 1.5-3.0 cm thick and shoot segments (5-7 cm long) were cut and then bark-peeled, placed immediately into glass vials and frozen in dry ice to avoid evaporation. Soil samples were collected for the same days at two depths (0–15 cm and ≈15–40 cm, that is, until reaching the bedrock) using a straight tube probe carefully cleaned between consecutive samplings. From 07:00 to 09:00 h solar time, samples were taken from soil pits located at intermediate positions between pairs of sampled D and ND individuals for each species. The soil extracted was placed rapidly into glass vials and frozen in dry ice. All samples were kept frozen until processing and analysis.

Xylem and soil water was extracted by cryogenic vacuum distillation (Martín-Gómez et al. 2015). Sample tubes were placed in a heated silicone oil bath (110–120°C), and connected with Ultra-Torr unions (Swagelok Co., Solon, OH, USA) to a vacuum system for a constant vacuum pressure of *ca*. 10^{-2} mbar, including U-shaped water traps in series that were refrigerated with liquid N_2. The extraction time was 90 min for xylem and 120 min for soil samples. Using exactly the same extraction device, this extraction time has been previously shown to be enough to extract all available water from similar soil and xylem samples (i.e., involving sub-mediterranean oaks) to those of our study (Martín-Gómez et al. 2017). Captured water was then transferred into cap-crimp 2-ml vials, and stored at 4°C until analysis. Gravimetric soil water content (GWC) was assessed for each sample using the sample weight before and after water extraction. A subset of representative samples, including both xylem and soil samples, was checked for complete water extraction by oven drying them at 105 °C for 36 h and

reweighing them. In all cases, the samples did not show a significant weight loss when placed in the drying oven.

The oxygen and hydrogen isotopic composition ($\delta^{18}O$ and $\delta^{2}H$, respectively) of water was determined by isotope ratio infrared spectroscopy (IRIS) using a Picarro L2120-i coupled to an A0211 high-precision vaporizer (Picarro Inc., Sunnyvale, CA, USA). The estimated precision, based on the repeated analysis of four reference water samples, was 0.10‰ for $\delta^{18}O$ and 0.40‰ for $\delta^{2}H$. Residual organic contaminants in the distilled water can hamper the interpretation of plant and soil water isotopic composition conducted with IRIS (Martín-Gómez et al., 2015). The occurrence of contaminants was tested using Picarro's CHEMCORRECT post-processing software and corrected, when necessary, following Martín-Gómez et al. (2015).

The local meteoric water line (LMWL) was obtained from rainfall isotope data collected in the Mt. Vulture volcano (40º 57' N, 15º 38' E), southern Italy, for the period 2002-2004 (Paternoster et al. 2008). LMWL was described as $\delta^{2}H = 3.72 + 6.44 \times \delta^{18}O$ (R^2=0.99). For groundwater, two alternative estimates were used: the weighted average of monthly isotopic signatures of precipitation from October to April (considered as the soil recharge period in the Mediterranean) at Mt. Vulture (within a 80-km radius from the experimental sites) over the same period using an available dataset built about 15 year ago (method 1), and the average of samples of water collected from seven (Gorgoglione) or five (San Paolo Albanese) nearby fountains or wells located within a 5-km radius of the sampled stands (method 2). These water samples were obtained at the end of June 2019. The results were as follows: -9.6 ± 0.94‰ (mean ± standard deviation) and -58.8 ± 9.17‰ (method 1), -7.7 ± 0.23‰ and -47.5 ± 1.21‰ (method 2, Gorgoglione), and -8.5 ± 0.17‰ and -51.8 ± 0.84‰ (method 2, San Paolo Albanese) for $\delta^{18}O$ and $\delta^{2}H$, respectively. The estimates of method 2 could

be influenced by the different origins of groundwater, either wells or fountains, the latter being prone to evaporative enrichment if water is openly exposed. A test for differences between the inferred isotopic compositions of groundwater depending on their origin (well or fountain) did not reveal a significant evaporative enrichment in samples originating from fountains (results not shown), which led us to use both water sources for groundwater estimation.

Evaporative enrichment of xylem water, which has a disproportionately greater effect on $\delta^{18}O$ than on $\delta^{2}H$ (Craig, 1961), was quantified through the concept of the soil water line-conditioned excess (SW-excess), as proposed by Barbeta et al. (2019). The SW-excess describes the potential offset of xylem water samples relative to their soil water line, and represents a modification of the line-conditioned excess (Landwehr and Coplen 2006), which in turn describes an offset of water samples relative to the LMWL. The SW-excess was computed as:

$$\text{SW-excess} = \delta^{2}H - a_S\delta^{18}O - b_S \quad [1]$$

where a_S and b_S are the slope and intercept, respectively, of the soil water line for a particular site and species, and $\delta^{2}H$ and $\delta^{18}O$ correspond to the isotopic composition of a xylem water sample collected on that site and species. The slope and intercept a_S and b_S were computed by performing a linear regression on all the soil water isotope data from the top and bottom horizons collected per site and species. The SW-excess has been recently used to quantify hydrogen isotope offsets occurring when $\delta^{2}H$ of xylem water is more depleted than the considered water sources (Barbeta et al. 2019), but its application is restricted to monotonic soil isotopic profiles. Negative SW-excess values indicate xylem samples that are more depleted in deuterium than the soil water line and are, thus, positioned below soil water samples in a $\delta^{18}O$ - $\delta^{2}H$ plot.

Non-structural carbohydrates (NSC) in sapwood

To assess the carbon status of coexisting ND and D trees we quantified sapwood NSC concentrations. We selected five trees per vigour class and sampled their sapwood at 1.3 m using Pressler increment borers (see Colangelo et al. 2017a). The sapwood was visually distinguished in the field and separated using a razor blade. Sapwood samples were collected in summer 2018, transported in a portable cooler to the laboratory, and stored at −20 °C until freeze-dried. Then, they were weighed and milled to a homogeneous powder in a ball mill (Retsch Mixer MM301, Leeds, UK). Soluble sugars were extracted with 80% (v/v) ethanol and their concentration was colorimetrically determined using the phenol-sulfuric method (Buysse and Merckx 1993). Starch and complex sugars remaining after ethanol extraction were enzymatically digested as described in Colangelo et al. (2017a). NSCs measured after ethanol extractions are referred to as soluble sugars (SS), and NSCs after enzymatic digestion are referred to as starch. Total NSC concentration (% dry matter) was calculated as the sum of SS and starch concentrations.

Statistical analyses

To compare variables between ND and D trees of each species (tree density, diameter at 1.3 m, height, age at 1.3 m, BAI, NSCs) and between soil depths (gravimetric soil water content) we used the Mann-Whitney *U* test. We tested if BAI of ND and D trees differed using the Wilcoxon rank-sum test because this statistic is robust against deviations from normality and autocorrelation (Hentschel et al. 2014).

For soil isotope records ($\delta^{18}O$ and $\delta^{2}H$), we fitted a two-way analysis of variance (ANOVA) considering sampled stand (*Q. cerris*, *Q. frainetto*, *Q. pubescens*) and soil depth (top, bottom) as main factors. For each sampled stand, we also fitted a

heterogeneity of slopes ANOVA to detect differences in the relative response of $\delta^{18}O$ to changes in $\delta^{2}H$ according to soil depth. To this end, the variability of $\delta^{18}O$ values was explained by soil depth, and $\delta^{2}H$ was introduced as covariable together with its interaction with soil depth.

For xylem isotope values ($\delta^{18}O$, $\delta^{2}H$ and SW-excess), we used a three-way ANOVA considering the following fixed factors and their interactions: species (*Q. cerris*, *Q. frainetto*, *Q. pubescens*), tree type (D, ND), and branch position (north, south). In addition, we allowed for heterogeneous residual variances at the tree type level. The better fit of this model compared with a model having homogeneous residuals was checked with AIC and BIC statistics. Mixed model ANOVAs were performed using the MIXED procedure of SAS/STAT v.9.4 (SAS Institute Inc., Cary, NC, USA).

Results

Tree size and radial growth

D and ND trees presented similar diameter and age irrespective of the oak species, but ND trees were significantly taller ($p<0.05$) than conspecific D trees, with differences ranging from 23% (*Q. cerris*) to 32% (*Q. frainetto* and *Q. pubescens*). These differences were not clearly related to stand density (Table 1). However, the density of D trees was significantly higher than that of ND trees in the case of *Q. cerris* and *Q. frainetto*.

The mean growth rate (BAI) of the last 25 years (period 1991-2016) was significantly higher in ND than in D trees for all species (Table 2). The relative growth reductions (BAI difference between ND and D trees) were 53.7%, 35.2 % and 42.0% in *Q. cerris*, *Q. frainetto* and *Q. pubescens*, respectively. For all oak species, ND trees grew more than D trees from 2002 to 2016, but this difference was also significant in

other previous periods, depending on each species (Table 2). Severe BAI reductions were observed in 1952, 1957, 1962, 1967, 1970, 1975, 1982-1983, 1990, 1995, 2002, and 2013 (Fig. 2). The recent divergence in growth between ND and D trees started in 2002 in the case of *Q. frainetto*, but higher growth rates in ND than in D trees could be traced back to 1953 in the other two species (Fig. 2, Table 2).

Differences in NSC between tree types

We found a significantly lower sapwood SS concentration in ND than in D trees of *Q. cerris* and *Q. frainetto*, but a higher starch concentration in ND trees of *Q. cerris* and *Q. pubescens* (Table 3). Total NSC concentration was lower in D trees of *Q. pubescens*, but higher in *Q. frainetto* D trees, with non-significant differences observed for *Q. cerris*.

Soil and xylem water isotopes

Top soil water was significantly more enriched than bottom soil water for both isotopes (p = 0.006 and 0.014 for $\delta^{18}O$ and $\delta^{2}H$, respectively) irrespective of sampled stand, denoting evaporative enrichment at the soil surface. There were also differences among stands for both isotopes ($p < 0.05$), with soil water of the *Q. pubescens* stand being significantly more enriched than that of *Q. frainetto*, hence suggesting higher soil evaporative enrichment for *Q. pubescens*, followed by *Q. cerris* and *Q. frainetto.* Except in very few cases, the soil water samples were consistently placed on the right side of the LMWL line, regardless of the sampled stand (Fig. 5, top panels).

The heterogeneity of slopes ANOVA did not detect differential soil evaporative enrichment as dependent on soil depth layer (i.e., different slopes conditional to soil depth), which indicated monotonic isotopic soil profiles across stands (slopes ranging

between 3.0 and 3.5; Fig. 5, top panels). These monotonic soil profiles may be related to the relatively shallow soils typical of these ecosystems. Consequently, direct evaporation may have exerted a similar effect across soil depths.

These soil slope values were significantly smaller than the slope of the LMWL line (6.4). The GWC did not significantly differ between soil depths for each sampled stand, with mean values of 10.4%, 11.1% and 12.2% for *Q. pubescens*, *Q. cerris* and *Q. frainetto*, respectively (Fig. 3a). Since soil physicochemical properties were approximately homogeneous across soil depths (e.g. pH = 7.6 ± 0.1 and 7.5 ± 0.2, EC = 182 ± 17 and 185 ± 37 µS cm^{-1} for top and bottom soil, respectively, at Gorgoglione), we estimated, based on the water retention properties of sandy loam soils, that the permanent wilting point was reached for roughly 30% of soil samples by end August. Top soil GWC was negatively correlated with soil water $\delta^{18}O$ across stands (r = -0.62; p = 0.01) but not with $\delta^{2}H$ (r= -0.42; p = 0.11). On the other hand, bottom soil GWC was unrelated to either $\delta^{18}O$ (r= -0.01; $p > 0.05$) or $\delta^{2}H$ (r= +0.17; $p > 0.05$).

For xylem isotopic composition, significant differences were observed among species for $\delta^{18}O$ and $\delta^{2}H$, and between tree types for $\delta^{18}O$ only (Table 4). However, there was a significant interaction between species and tree type for both isotopes. Declining trees of *Q. pubescens* and *Q. cerris* showed significantly higher $\delta^{18}O$ values than ND trees, whereas both tree types had statistically similar $\delta^{18}O$ values for *Q. frainetto* (Fig. 4a). Also, D trees had significantly higher $\delta^{2}H$ values than ND trees for *Q. pubescens*, although non-significant differences were found for *Q. cerris* and statistically higher $\delta^{2}H$ values of ND trees were observed for *Q. frainetto* (Fig. 4b). Despite such differences, the ranking of species was consistent across tree types, with *Q. pubescens* showing the least negative values, followed by *Q. cerris* and, finally, *Q. frainetto*. There were neither significant differences between branch positions nor

significant interactions involving this factor, suggesting lack of differential access to water sources across the tree crown.

Visual inspection of the xylem water samples in the dual-isotope space indicated that the isotopic signatures of the oak trees clearly departed from the LMWL line and, also, from the isotopic soil water evaporation lines (Fig. 5, bottom panels). In particular, xylem water samples had consistently more depleted δ^2H values than top and bottom soil layers ($p < 0.001$) for all oak species. Hence, xylem samples fell outside the range of the monitored water sources in the dual-isotope space, including groundwater estimated from natural springs (Fig. 5, bottom panels). For most sampled stands, the lower part of the isotopic soil water evaporation line crossed the LMWL line at the exact position of the natural spring-based groundwater estimate in the dual-isotope space. The exception was the *Q. pubescens* stand, in which the isotopic soil water evaporation line crossed the LMWL line close to the position of the precipitation-based groundwater estimate.

According to soil water $\delta^{18}O$ alone, the oak trees mainly took up water from deep soil sources (bottom soil or groundwater), irrespective of oak species. This was suggested by xylem water $\delta^{18}O$ values that were intermediate between the bottom soil and the groundwater $\delta^{18}O$ values in most cases (Fig. 5, bottom panels). However, the xylem water of *Q. pubescens* and *Q. cerris* was closer to the bottom soil values (15-40 cm), especially in the case of declining trees. On the other hand, the xylem water of *Q. frainetto* took values across the range of values of the bottom soil and the groundwater but closer to groundwater, without obvious differences between D and ND trees.

The isotopic offset between xylem and soil water samples was examined through calculation of the SW-excess. Overall, the SW-excess was significantly larger in *Q. cerris* (SW-excess = -10.27 ± 3.5; mean ± SD) and *Q. frainetto* (-11.89 ± 1.6) compared

with *Q. pubescens* (-7.1 ± 1.7) (Fig. 3b), but non-significant effects of tree type and of the interaction between tree type and species were observed (Table 4). Moreover, we did not find significant effects associated with branch position or its interaction with tree type and species.

Discussion

As hypothesized, our results indicate than non-declining oak trees of *Q. cerris* and *Q. pubescens* extracted deeper soil water than declining trees during peak summer, suggesting the existence of tree-to-tree variability in root access to different soil layers. The exception to this pattern was *Q. frainetto*. For this species, D and ND conspecifics likely drew the same deep water using a similar survival strategy to that of the ND individuals in *Q. cerris* and *Q. pubescens*, despite *Q. frainetto* is mainly found in mesic Mediterranean sites with *a priori* less requirements on preferential access to deeper water. On the other hand, we did not find support for our second hypothesis stating that declining trees should show a lower total NSC concentration than non-declining trees regardless of species, which could be indicative of carbon starvation as die-back mechanism (*cf*. McDowell et al. 2008).

Mediterranean oaks can keep their physiological activity during summer by relying on water reservoirs like groundwater or deep soil layers (Del Castillo et al. 2016, Martín-Gómez et al. 2017). A strong dependence of deciduous oaks on rainfall recharge during autumn and winter has been observed in the western Mediterranean basin through the analysis of stable oxygen isotopes in wood cellulose (Shestakova et al. 2014). In this regard, the differences between declining and non-declining trees were only evident for the more xeric species, which reinforces the importance of the reliance on deep soil water pools of oaks for survival under progressively hotter droughts.

However, we observed a clear isotopic offset between soil and xylem water isotopes in peak summer regardless of the species. For this reason, we could not quantify the relative contribution of different soil depths as water sources for declining and non-declining trees using a mixing model (e.g. Voltas et al. 2015).

In fact, the xylem samples were placed along an alternative evaporation line of soil water that may correspond to previous months of the growing season, as previously reported for *Q. ilex* subjected to an acute drought (Del Castillo et al. 2016). This might indicate that both tree types were not actively taking up water in peak summer, therefore ceasing their physiological activity (i.e. transpiration) during the extreme summer drought of 2017. This is feasible taking into account that there was 0 mm of precipitation in July and August 2017, and the precipitation for the first half of the year was only 61% of a normal year. The low soil GWC also points in this direction. The analysis of seasonal dynamics of root access to different water pools would provide additional clues on the physiological performance of healthy and declining oak trees, as demonstrated for understanding differences among functional types in drought-prone environments (Barbeta et al. 2015; Martín-Gómez et al. 2017; Antunes et al. 2018).

The isotopic offset between xylem and soil water samples, however, does not necessarily indicates an older age of water kept by the trees in peak summer. Indeed, there is a growing body of literature reporting on deuterium fractionation in controlled experiments (Vargas et al. 2017) or natural conditions (Evaristo and McDonnell 2017, Barbeta et al. 2019, Oerter and Bowen 2019), either under full irrigation or drought stress. Consequently, a number of alternative but non-exclusive explanations have been raised to explain isotope offsets occurring when xylem water is more ^{2}H-depleted than the considered water sources. Amongst them, root discrimination against the heavier ^{2}H may occur in the unsaturated soil-root interface following vapour condensation, a

process becoming progressively more important as soil dries out (Vargas et al. 2017, Barbeta et al. 2019). This challenges the general assumption of lack of fractionation during root water uptake (Lin and Sternberg 1993). Also, spatial heterogeneity in the stable isotopic composition of soil water with different mobility may also impact on xylem isotopic signatures (Orlowski et al. 2018, Dubbert et al. 2019, Oerter and Bowen 2019), thereby complicating tree water source identification. Deuterium fractionation has also been reported between xylem sap and root or stem tissue water in drylands (Zhao et al. 2016), and water cycling, storage and exchange is known to be more common than previously assumed in plants, which together could change xylem isotopic composition. We can neither discard the influence of cavitation processes for anisohydric species, such as oaks, on the explanation of the offset in xylem isotopic composition. In fact, xylem water sampling took place at noon solar time during peak summer, which may have increased the risk of cavitation and hydraulic failure in the sampled trees, thereby mediating the water exchange between phloem and xylem due to embolism repair and, hence, the observed xylem offset (Nardini et al. 2011, Pfautsch et al. 2015). The rock permeability of the area, which can create differences in exchangeable water held in weathered bedrock, has been also postulated as an alternative source of water for plants that might explain isotopic offsets (Palacio et al. 2014, Oshun et al. 2015, Barbeta & Peñuelas 2017, Rempe & Dietrich 2018).

A role of mycorrhizal fungi on the preferential uptake of the light hydrogen isotope by plants has been also proposed (Poca et al. 2019), again questioning the fractionation-free assumption during root water uptake. Since free-living fungi and mycorrhizal species are negatively affected by drought (Castaño et al. 2018), the extent of root discrimination against the heavier ^{2}H is expected to be relatively more important under optimal soil water conditions. In fact, the stand most affected by drought (*Q.*

pubescens) showed a significantly higher (i.e., less negative) SW-excess, which suggests potential effects of soil fungi on tree water uptake being more important in less water-limited sites (Rempe and Dietrich 2018). Regardless of the relative magnitude of deuterium fractionation processes, the closer values of xylem water to groundwater in non-declining trees of *Q. cerris* and *Q. pubescens* point to a preferential access to deep water reservoirs for healthy individuals of these species.

Only declining trees of *Q. pubescens*, the species dominant under the most xeric conditions of our study and which better tolerates drought (Tognetti et al. 1998), presented a lower NSC concentration than non-declining trees. Conversely, *Q. cerris* trees of different vigor presented a similar total NSC concentration. In fact, starch concentration was significantly lower in declining trees of *Q. cerris*, but SS concentration was higher in declining trees of the same species. In the case of *Q. frainetto*, declining trees showed a significantly higher total NSC concentration than non-declining individuals (Colangelo et al. 2017a). In this species, declining trees, which also showed lower recent growth rates than non-declining trees, may be storing carbon not used for producing stem wood as sapwood NSCs, in agreement with previous theoretical (Tardieu et al. 2011, Körner 2013) and empirical evidences (Muller et al. 2011). These studies emphasize that carbon sinks (e.g., cambium and leaf growth) are much more sensitive to water deficit (i.e., their activity is restricted earlier or at lower levels of drought stress) than carbon sources (e.g., photosynthesis rate). Furthermore, the higher concentrations of soluble sugars in declining trees of *Q. cerris* and *Q. frainetto* could be due to their role as osmolytes or to impaired phloem functioning which prevents access to carbohydrate reserves (Sala et al. 2012).

However, these measured differences in NSC pools between declining and non-declining trees in *Q. pubescens* and *Q. frainetto* may have been also affected by

different water availability in summer across years. Indeed the tree-ring width data show that the differences between declining and non-declining trees arose much before the sampling date, especially in *Q. pubescens*. Of course, these prior (chronic) differences in growth may be due to several reasons (i.e. previous dieback episodes, disturbances, selective dead of trees with lowest growth rates, etc.), and may have differently predisposed trees to the 2010s droughts. However, non-declining and declining trees showed similar growth rates during dry periods (Fig. 2), whereas non-declining trees grew more than declining trees during wet years, except for *Q. frainetto* where declining trees displayed a higher BAI than non-declining trees around 1960s. These shifting responses indicate a reduced responsiveness to water shortage during that cool period which could explain the higher growth rate of declining trees. However, we cannot discard other potential drivers explaining the differences in growth rates including management, pests, fire or other climatic events (e.g., frosts, etc.). Such different growth responsiveness to drought and temperature variation can predispose trees to show decline in response to recent droughts and reconcile observations made at decadal to annual scales.

As previously observed (Colangelo et al. 2017b), declining trees were shorter than non-declining trees, regardless of species. This difference cannot be fully explained by changes in tree-to-tree competition intensity. Recently, declining trees also showed lower radial growth rates, thus reducing their sapwood cross-sectional area which would disproportionally affect their leaf and root production (Magnani et al. 2000). This could have magnified the disparity in scaling strategies between declining and non-declining trees leading to an irreversible drought-induced reduction in radial growth, hydraulic conductivity and carbon uptake. How successive and hotter droughts contribute to sharp

growth reductions and increased differences in vulnerability within a tree species is still unclear.

Tree-to-tree size variability could be connected to the observed differences in access to deep water pools since shorter declining trees could form shallower or less efficient root systems, thus relying more on superficial soil water than taller, deep-rooted, non-declining trees. Such allometric or scaling relationships (*cf*. Ledo et al. 2018) are understudied in the case of drought-induced dieback, and demand further research to assess how allocation patterns (i.e., root to shoot ratio) drive access to soil water and if these relationships are related to drought damage at the intra-specific level. Similar approaches have been carried out for interspecific comparisons (Olson et al. 2018). For example, large trees might form more extensive and deeper root systems or have a higher hydraulic capacitance (Bucci et al. 2005), and thus show a better capacity to tolerate drought stress. The assignment of such differences to adaptive variation in the responses to drought should also consider confounding factors as microsite differences (e.g., topography-mediated hydrologic refugia) or climate-driven changes in root to shoot ratios (e.g., Camarero et al. 2016, 2018).

The idea that declining trees may be less able to access to deep water pools than non-declining trees is supported by empirical studies. In an experimental setting where dry and warm conditions were induced, drought led to deeper water uptake in stressed trees relative to ambient, unstressed trees (Grossiord et al. 2017). Such shift in water uptake depth can be linked to a higher carbon allocation to deep roots under conditions of soil water depletion or elevated VPD during the dry summer (Bréda et al. 2006). This seasonal shift can disappear when precipitation increases and water sources from shallower soil layers become fully available (Voltas et al. 2015). In addition, the ability of roots to uptake increasing amounts of groundwater with extended and hotter droughts

is limited (Markewitz et al. 2010, Barbeta et al. 2015), and high soil temperature may restrain root activity and water and nutrients uptake in species with shallow roots or amplify soil hydrophobicity (Williams and Ehleringer 2000). Local factors like the differential access to deep water sources should be included in models to produce more realistic forecasts of forest dieback. Soil factors could explain why drought triggers dieback in sites where that was not an *a priori* expectation (Gazol et al. 2018).

Conclusions

We investigated tree-to-tree variability of radial growth, soil water uptake and NSC concentrations in three oak species showing drought-induced dieback. In peak summer, non-declining trees extracted deeper soil water than declining trees in *Q. cerris* and *Q. pubescens*, as indicated by significantly more depleted xylem water values, but this was not the case in *Q. frainetto*, a species which dominates in mesic sites. The evidence for deuterium fractionation taking place at the soil or plant level, however, prevented a proper quantification of the relevance of different water pools for tree transpiration. Declining trees showed lower height and radial-growth rate than non-declining trees. Sapwood starch concentrations were lower in declining trees in *Q. cerris* and *Q. pubescens*. To the extent of our knowledge, this is the first study showing how the differential access to deep water reservoirs influences drought-induced decay of individuals of a species population subjected to a dieback episode. Additional work should focus on the investigation of seasonal dynamics of water use, reserves and other physiological indicators (i.e., stable isotopes in dry matter) related to potential differences in water uptake capacity within the soil profile between healthy and declining trees.

Acknowledgements

This research was financially supported by the project OT4CLIMA (Italian Ministry of Education, Universities and Research – MIUR ARS01_00405) "Advanced EO Technologies for studying climate change impacts on the environment" and by the project "Alarm of forest mortality in Southern Italy" (Gorgoglione Administration, Basilicata Region, Italy). MC was supported by the PhD program from the University of Basilicata (Italy). JJC acknowledges funding by the project CGL2015-69186-C2-1-R project (Spanish Ministry of Economy). We acknowledge the E-OBS dataset from the EU-FP6 project UERRA (http://www.uerra.eu) and the data providers in the ECA&D project (https://www.ecad.eu).

References

Adams HD, Zeppel MJB, Anderegg WRL, Hartmann H, Landhäusser S, Tissue DT, Huxman TE, Hudson PJ, Franz TE, Allen CD, Anderegg LDL, Barron-Gafford GA, Beerling DJ, Breshears DD, Brodribb TJ, Bugmann H, Cobb RC, Collins AD, Dickman LT, Duan H, Ewers BE, Galiano L, Galvez DA, Garcia-Forner N, Gaylord ML, Germino MJ, Gessler A, Hacke UG, Hakamada R, Hector A, Jenkins MW, Kane JM, Kolb TE, Law DJ, Lewis JD, Limousin J-M, Love DM, Macalady AK, Martínez-Vilalta J, Mencuccini M, Mitchell PJ, Muss JD, O'Brien MJ, O'Grady AP, Pangle RE, Pinkard EA, Piper FI, Plaut JA, Pockman WT, Quirk J, Reinhardt K, Ripullone F, Ryan MG, Sala A, Sevanto S, Sperry JS, Vargas R, Vennetier M, Way DA, Xu C, Yepez EA, McDowell NG (2017) A multi-species synthesis of physiological mechanisms in drought-induced tree mortality. Nat Ecol Evol 1: 1285–1291.

Allen CD, Breshears DD, McDowell NG (2015) On underestimation of global vulnerability to tree mortality and forest die-off from hotter drought in the Anthropocene. Ecosphere 6: art129.

Anderegg WRL, Klein T, Bartlett M, Sack L, Pellegrini AF, Choat B, Jansen S (2016) Meta-analysis reveals that hydraulic traits explain cross-species patterns of drought-induced tree mortality across the globe. PNAS 113: 5024–5029.

Anderegg WRL, Konings AG, Trugman AT, Yu K, Bowling DR, Gabbitas R, Karp DS, Pacala S, Sperry JS, Sulman BN, Zenes N (2018) Hydraulic diversity of forests regulates ecosystem resilience during drought. Nature 561: 538–541.

Antunes C, Chozas S, West J, Zunzunegui M, Diaz Barradas MC, Vieira S, Máguas C (2018) Groundwater drawdown drives ecophysiological adjustments of woody vegetation in a semi-arid coastal ecosystem. Glob Ch Biol 24: 4894–4908.

Barbeta A, Mejía-Chang M, Ogaya R, Voltas J, Dawson TE, Peñuelas J (2015) The combined effects of a long-term experimental drought and an extreme drought on the use of plant-water sources in a Mediterranean forest. Glob Ch Biol 21: 1213–1225.

Barbeta A, Peñuelas J (2017) Relative contribution of groundwater to plant transpiration estimated with stable isotopes. Sci reports 7: 10580.

Barbeta A, Jones SP, Clavé L, Wingate L, Gimeno TE, Fréjaville B, Wohl S, Ogée J (2019) Unexplained hydrogen isotope offsets complicate the identification and quantification of tree water sources in a riparian forest. Hydrol Earth Syst Sci 23: 2129–2146.

Bréda N, Huc R, Granier A, Dreyer E (2006) Temperate forest trees and stands under severe drought: a review of ecophysiological responses, adaptation processes and long-term consequences. Ann For Sci 63: 625–644.

Bucci SJ, Goldstein G, Meinzer FC, Franco AC, Campanello P, Scholz FG (2005) Mechanisms contributing to seasonal homeostasis of minimum leaf water potential and predawn disequilibrium between soil and plant water potential in Neotropical savanna trees. Trees 19: 296–304.

Buysse J, Merckx R (1993) An improved colorimetric method to quantify sugar content of plant tissue. J Exp Bot 44: 1627–1629.

Cailleret M, Dakos V, Jansen S, Robert EMR, Aakala T, Amoroso MM, Antos JA, Bigler C, Bugmann H, Caccianaga M, Camarero JJ, Cherubini P, Coyea MR, Čufar K, Das AJ, Davi H, Gea-Izquierdo G, Gillner S, Haavik LJ, Hartmann H, Hereş A-M, Hultine KR, Janda P, Kane JM, Kharuk VI, Kitzberger T, Klein T, Levanic T, Linares J-C, Lombardi F, Mäkinen H, Mészáros I, Metsaranta JM, Oberhuber W, Papadopoulos A, Petritan AM, Rohner B, Sangüesa-Barreda G,

Smith JM, Stan AB, Stojanovic DB, Suarez M-L, Svoboda M, Trotsiuk V, Villalba R, Westwood AR, Wyckoff PH, Martínez-Vilalta J (2018) Early-warning signals of individual tree mortality based on annual radial growth. Front. Plant Sci., https://doi.org/10.3389/fpls.2018.01964

Camarero JJ, Gazol, A., Sangüesa-Barreda, G., Oliva, J. and Vicente-Serrano, S. M. 2015. To die or not to die: early-warning signals of dieback in response to a severe drought. J Ecol 103: 44–57.

Camarero JJ, Sangüesa-Barreda G, Vergarechea M (2016) Prior height, growth, and wood anatomy differently predispose to drought-induced dieback in two Mediterranean oak species. Ann For Sci 73: 341–351.

Camarero, JJ, Sánchez-Salguero, R, Sangüesa-Barreda G, Matías L (2018). Tree species from contrasting hydrological niches show divergent growth and water-use efficiency. Dendrochronologia 52: 87–95.

Castaño C, Lindahl BD, Alday JG, Hagenbo A, Martínez de Aragón J, Parladé J, Pera J, Bonet JA (2018) Soil microclimate changes affect soil fungal communities in aMediterranean pine forest. New Phytol 220: 1211–1221.

Chitra-Tarak R, Ruiz L, Dattaraja H S, Kumar MSM, Riotte J, Suresh HS, McMahon SM, Sukumar R (2018) The roots of the drought: hydrology and water uptake strategies mediate forest-wide demographic response to precipitation. J Ecol 106: 1495–1507.

Choat B, Brodribb TJ, Brodersen CR, Duursma RA, López R, Medlyn BE (2018) Triggers of tree mortality under drought. Nature 558: 531–539.

Colangelo M, Camarero JJ, Battipaglia G, Borghetti M, De Micco V, Gentilesca T, Ripullone F (2017°) A multi-proxy assessment of dieback causes in a Mediterranean oak species. Tree Physiol 37: 617-631

Colangelo M, Camarero JJ, Borghetti M, Gazol A, Ripullone F (2017b) Size matters a lot: drought-affected Italian oaks are smaller and show lower growth prior to tree death. Front Plant Sci 8: 135.

Colangelo M, Camarero JJ, Borghetti M, Gentilesca T, Oliva J, Ripullone F, Redondo MA (2018) Drought and *Phytophthora* are associated with the decline of oak species in southern Italy. Fron Plant Sci 9: 1595.

Cornes, R., G. van der Schrier, E.J.M. van den Besselaar, and P.D. Jones. (2018) An ensemble version of the E-OBS temperature and precipitation datasets. J. Geophys. Res. Atmos., 123: 9391-9409. doi:10.1029/2017JD028200.

Costa A, Pereira H, Madeira M (2010) Analysis of spatial patterns of oak decline in cork oak woodlands in Mediterranean conditions. Ann For Sci 67: 204.

Del Castillo J, Comas C, Voltas J, Ferrio JP (2016) Dynamics of competition over water in a mixed oak-pine Mediterranean forest: Spatio-temporal and physiological components. For Ecol Manage 382: 214–224.

Dubbert M, Werner C (2019) Water fluxes mediated by vegetation: emerging isotopic insights at the soil and atmosphere interfaces. New Phytol 221: 1754–1763.

Dubbert M, Caldeira MC, Dubbert D, Werner C (2019) A pool-weighted perspective on the two-water-worlds hypothesis. New Phytol 222: 1271–1283.

Duncan RP. 1989. An evaluation of errors in tree age estimates based on increment cores in Kahikatea *(Dacrycarpus* dacrydiodes). New Zealand Nat Sci 16: 31–37.

Ehleringer JR, Dawson TE (1992) Water uptake by plants: perspectives from stable isotope composition. Plant, Cell Env 15: 1073–1082.

Evaristo J, McDonnel JJ (2017) Prevalence and magnitude of groundwater use by vegetation: a global stable isotope meta-analysis. Sci. Reports 7:44110.

Gärtner H, Nievergelt D (2010) The core-microtome: a new tool for surface preparation on cores and time series analysis of varying cell parameters. Dendrochronologia 28: 85–92.

Gazol A, Camarero JJ, Jiménez JJ, Moret-Fernández D, López MV, Sangüesa-Barreda G, Igual JM. 2018. Beneath the canopy: linking drought-induced forest die off and changes in soil properties. For Ecol Manage 422: 294–302.

Gentilesca T, Camarero JJ, Colangelo M, Nolè A, Ripullone F (2017) Drought-induced oak decline in the western Mediterranean region: an overview on current evidences, mechanisms and management options to improve forest resilience. iForests 10: 796–806.

Greenwood S, Ruiz-Benito P, Martínez-Vilalta J, Lloret F, Kitzberger T, Allen CD, Kraft NJ (2017) Tree mortality across biomes is promoted by drought intensity, lower wood density and higher specific leaf area. Ecol Lett 20: 539–553.

Grossiord C, Sevanto S, Dawson TE, Adams HD, Collins AD, Dickman LT, Newman BD, Stockton EA, McDowell NG (2017) Warming combined with more extreme precipitation regimes modifies the water sources used by trees. New Phytol 213: 584–596.

Hasselquist NJ, Allen MF, Santiago LS (2010) Water relations of evergreen and drought-deciduous trees along a seasonally dry tropical forest chronosequence. Oecologia 164: 881–890.

Hentschel R, Rosner S, Kayler ZE, Andreassen K, Børja I, Solverg S, Tveito OE, Priescak E, Gessler A (2014) Norway spruce physiological and anatomical predisposition to dieback. For Ecol Manage 322: 27–36.

Holmes RL (1983) Computer-assisted quality control in tree-ring dating and measurement. Tree-Ring Res 43: 69–78.

Johnson DM, Domec JC, Carter Berry Z, Schwantes AM, McCulloh KA, Woodruff DR, Wayne Polley H, Wortemann R, Swenson JJ, Scott Mackay D, McDowell NG, Jackson RB (2018) Co-occurring woody species have diverse hydraulic strategies and mortality rates during an extreme drought. Plant Cell Env 41: 576–88.

Javaux M, Rothfuss Y, Vanderborght J, Vereecken H, Brüggemann N (2016) Isotopic composition of plant water sources. Nature 536 E1-E3.

Klein T (2014) The variability of stomatal sensitivity to leaf water potential across tree species indicates a continuum between isohydric and anisohydric behaviours. Funct Ecol 28: 1313–1320.

Körner C (2013) Growth controls photosynthesis – mostly. Nova Acta Leopoldina 114: 273–283.

Ledo A, Paul KI, Burslem DF, Ewel JJ, Barton C, Battaglia M, Brooksbank K, Carter J, Eid TH, England JR, Fitzgerald A, Jonson J, Mencuccini M, Montagu KD, Montero G, Mugasha WA, Pinkard E, Roxburgh S, Ryan CM, Ruiz-Peinado R, Sochacki S, Specht A, Wildy D, Wirth C, Zerihun A, Chave J (2018) Tree size and climatic water deficit control root to shoot ratio in individual trees globally. New Phytol 217: 8–11.

Lin G, Sternberg LSL (1993) Hydrogen isotopic fractionation by plant roots during water uptake in coastal wetland plants. In: Ehleringer J, Hall A, Farquhar G, eds. Stable isotopes and plant carbon-water relations. New York: Academic Press Inc., 497–510.

Liu H, Gleason SM, Hao G, Hua L, He P, Goldstein G, Ye G (2019) Hydraulic traits are coordinated with maximum plant height at the global scale. Sci. Adv. 5: eaav1332.

Magnani F, Mencuccini M, Grace J (2000) Age-related decline in stand productivity: the role of structural acclimation under hydraulic constraints. Plant Cell Env 23: 251–263.

Markewitz D, Devine S, Davidson EA, Brando P, Nepstad DC (2010) Soil moisture depletion under simulated drought in the Amazon: Impacts on deep root uptake. New Phytol 187: 592–607.

Martín-Gómez P, Barbeta A, Voltas J, Peñuelas J, Denis K, Palacio S, Dawson TE, Ferrio JP (2015) Isotope ratio infrared spectroscopy: a reliable tool for the investigation of plant-water sources? New Phytol 207: 914–927.

Martín-Gómez P, Serrano L, Ferrio JP (2017a) Short-term dynamics of evaporative enrichment of xylem water in woody stems: implications for ecohydrology. Tree Physiol 37: 511-522.

Martín-Gómez P, Aguilera M, Pemán J, Gil-Pelegrín E, Ferrio JP (2017b) Contrasting ecophysiological strategies related to drought: the case of a mixed stand of Scots pine (*Pinus sylvestris*) and a submediterranean oak (*Quercus subpyrenaica*). Tree Physiol 37: 1478–1492.

Martin-StPaul N, Delzon S, Cochard H (2017) Plant resistance to drought depends on timely stomatal closure. Ecol Lett 20: 1437–1447.

McDowell NG, Pockman WT, Allen CD, Breshears DD, Cobb N, Kolb T, Plaut J, Sperry JS, West A, Williams DG, Yepez EA (2008) Mechanisms of plant survival and mortality during drought: why do some plants survive while others succumb to drought? New Phytol 178: 719–739.

McDowell NG, Allen CD (2015) Darcy's law predicts widespread forest mortality under climate warming. Nat Clim Ch 5: 669–672.

McLaughlin BC, Ackerly DD, Klos PZ, Natali J, Dawson TE, Thompson SE (2017) Hydrologic refugia, plants, and climate change. Glob Ch Biol 23: 2941–2961.

Meinzer FC, Andrade JL, Goldstein G, Holbrook NM, Cavelier J, Wright SJ (1999) Partitioning of soil water among canopy trees in a seasonally dry tropical forest. Oecologia 121: 293–301.

Moreno-Gutierrez C, Dawson TE, Nicolas E, Querejeta JI (2012). Isotopes reveal contrasting water use strategies among coexisting plant species in a Mediterranean ecosystem. New Phytol 196: 489–496.

Muller B, Pantin F, Génard M, Turc O, Freixes S, Piques M, Gibon Y (2011) Water deficits uncouple growth from photosynthesis, increase C content, and modify the relationships between C and growth in sink organs. J Exp Bot 62: 1715–1729.

Nardini A, Lo Gullo MA, Salleo S (2011) Refilling embolized xylem conduits: is it a matter of phloem unloading? Plant Sci 180(4), 604-611.

Nardini A, Battistuzzo M, Savi T (2013) Shoot desiccation and hydraulic failure in temperate woody angiosperms during an extreme summer drought. New Phytol 200: 322–329.

Oerter EJ, Bowen GJ (2019) Spatio-temporal heterogeneity in soil water stable isotopic composition and its ecohydrologic implications in semi-arid ecosystems. Hydrol Process 33: 1724–1738.

Olson ME, Soriano D, Rosell JA, Anfodillo T, Donoghue MJ, Edwards EJ, León-Gómez C, Dawson T, Camarero JJ, Castorena M, Echeverría A, Espinosa CI, Fajardo A, Gazol A, Isnard S, Lima RS, Marcati CR, Méndez-Alonzo R (2018)

Plant height and hydraulic vulnerability to drought and cold. PNAS 115: 7551–7556.

Orlowski N, Breuer L, Angeli N, Boeckx P, Brumbt C, Cook CS, Dubbert M, Dyckmans J, Gallagher B, Gralher B, Herbstritt B, Hervé-Fernández P, Hissler C, Koeniger P, Legout A, Joan Macdonald C, Oyarzún C, Redelstein R, Seidler C, Siegwolf R, Stumpp C, Thomsen S, Weiler M, Werner C, McDonnell JJ (2018) Inter-laboratory comparison of cryogenic water extraction systems for stable isotope analysis of soil water. Hydrol Earth Syst Sci 22: 3619–3637.

Otieno DO, Kurz-Besson C, Liu J, Schmidt MWT, Vale-Lobo d, David TS, Siegwolf R, Pereira JS, Tenhunen JD (2006) Seasonal variations in soil and plant water status in a *Quercus suber* L. stand: roots as determinants of tree productivity and survival in the Mediterranean-type ecosystem. Plant Soil 283: 119–135

Dinamic, structured heterogeneity of water isotopes inside hillslopes (2015) Oshun J, Dietrich WE, Dawson TE, Fung I Water Resource Res 52(1): 4840–4847.

Padilla FM, Pugnaire FI (2007) Rooting depth and soil moisture control Mediterranean woody seedling survival during drought. Funct Ecol 21: 489–495.

Palacio S, Azorin J, Montserrat-Martì G, Ferrio JP (2014) The crystallization water of gypsum rocks is a relevant water source for plants. Nature Commun 5: 4660.

Paternoster M, Liotta M, Favara R (2008) Stable isotope ratios in meteoric recharge and groundwater at Mt. Vulture volcano, southern Italy. J Hydrol 348: 87–97.

Pfautsch S, Renard J, Tioelker MG, Salih A (2015) Phloem as Capacitor: Radial Transfer of Water into Xylem of Tree Stems Occurs via Symplastic Transport in Ray Parenchyma. Plant Physiol 167(3): 963–971.

Pinheiro HA, DaMatta FM, Chaves AR, Loureiro ME, Ducatti C (2005) Drought tolerance is associated with rooting depth and stomatal control of water use in clones of *Coffea canephora*. Ann Bot 96: 101-108.

Pivovaroff AL, Pasquini SC, De Guzman ME, Alstad KP, Stemke JS, Santiago LS (2016) Multiple strategies for drought survival among woody plant species. Funct Ecol 30: 517–526.

Poca M, Coomans O, Urcelay C, Zeballos SR, Bodé S, Boecks P (2019) Isotope fractionation during root water uptake by *Acacia caven* is enhanced by arbuscular mycorrhizas. Plant Soil 441: 485–497.

Rempe DM and Dietrich WE (2018) Direct observations of rock moisture, a hidden component of the hydrologic cycle. Proc Natl Acad Sci 115(11): 2664–2669.

Sala A, Woodruff DR, Meinzer FC (2012) Carbon dynamics in trees: feast or famine? Tree Physiol 32: 764–775.

San-Miguel-Ayanz J, de Rigo D, Caudullo G, Houston Durrant T, Mauri A (Eds.) (2016) European Atlas of Forest Tree Species. European Union, Luxembourg.

Sánchez-Salguero R, Camarero JJ, Carrer M, Gutiérrez E, Alla AQ, Andreu-Hayles L, Hevia A, Koutavas A, Martínez-Sancho E, Nola P, Papadopoulos A, Pasho E, Toromani E, Carreira JA, Linares JC (2017) Climate extremes and predicted warming threaten Mediterranean Holocene fir forests refugia. PNAS 14: E10142–E10150.

SAS (2015) SAS Institute Inc. SAS/STAT®14.1 User's Guide. Cary, NC, USA.

Shestakova TA, Aguilera M, Ferrio JP, Gutiérrez E, Voltas J (2014) Unravelling spatiotemporal tree-ring signals in Mediterranean oaks: a variance–covariance modelling approach of carbon and oxygen isotope ratios. Tree Physiol 34: 819–838.

Tardieu F, Granier C, Muller B (2011) Water deficit and growth. Co-ordinating processes without an orchestrator? Curr Opinion in Plant Biol 14: 283–289.

Tognetti R, Longobucco A, Raschi A (1998) Vulnerability of xylem to embolism in relation to plant hydraulic resistance in *Quercus pubescens* and *Quercus ilex* co-occurring in a Mediterranean coppice in central Italy. New Phytol 139: 437–447.

Vargas AI, Schaffer B, Yuhong L, Sternberg LSL (2017) Testing plant use of mobile vs immobile soil water sources using stable isotope experiments. New Phytol 215: 582–594.

Voltas J, Camarero JJ, Carulla D, Aguilera M, Ortiz A, Ferrio JP (2013) A retrospective, dual-isotope approach reveals individual predispositions to winter-drought induced tree dieback in the southernmost distribution limit of Scots pine. Plant Cell Environ 36: 1435–1448.

Voltas J, Lucabaugh D, Chambel MR, Ferrio JP (2015) Intraspecific variation in the use of water sources by the circum-Mediterranean conifer *Pinus halepensis*. New Phytol 208: 1031–1041.

Wells N, Goddard S and Hayes MJ (2004) A self-calibrating Palmer Drought Severity Index. J Clim 17: 2335-2351.

Williams DG, Ehleringer JR (2000) Intra- and interspecific variation for summer precipitation use in pinyon–juniper woodlands. Ecol Monogr 70: 517–537.

Zhao L, Wang L, Cernusak LA, Liu X, Xiao H, Zhou M, Zhang S (2016) Significant difference in Hydrogen isotope composition between xylem and tissue water in *Populus euphratica*. Plant Cell Environ 39: 1848–1857.

Tables

Table 1. Main structural characteristics of the declining (D) and non-declining (ND) trees of the three study oak species (*Q. pubescens, Q. cerris*, and *Q. frainetto*). Values are means ± SE. Different letters indicate significant differences at the 0.05 level based on Mann-Whitney tests.

Tree species	Vigor class	Density (trees ha^{-1})	Diameter at 1.3 m (cm)	Height (m)	Age at 1.3 m (years)
Quercus pubescens	D	83 ± 6a	24.7 ± 0.7a	8.6 ± 0.3a	110 ± 3a
	ND	100 ± 11a	25.8 ± 0.9a	11.3 ± 0.3b	115 ± 4a
Quercus cerris	D	262 ± 16b	29.3 ± 0.8a	12.2 ± 0.4a	107 ± 2a
	ND	148 ± 13a	32.0 ± 0.9a	15.0 ± 0.6b	102 ± 4a
Quercus frainetto	D	244 ± 14b	29.9 ± 1.2a	10.2 ± 0.3a	132 ± 4a
	ND	104 ± 12a	31.9 ± 1.4a	13.5 ± 0.5b	140 ± 5a

Table 2. Comparisons of radial-growth rates (BAI, basal area increment) between coexisting non-declining (ND) and declining (D) trees of the three study oak species. Values are means ± SE. Different letters among BAI averages indicate significant differences at the 0.05 level based on Mann-Whitney tests. The lowermost row shows periods when ND trees grew significantly ($p < 0.05$) more than D trees according to Wilcoxon rank-sum tests.

	Quercus cerris	*Quercus frainetto*	*Quercus pubescens*
Mean BAI ND trees 1991- 2016 (mm^2)	884.26 ± 63.86b	655.99 ± 26.82b	448.51 ± 17.48b
Mean BAI D trees 1991- 2016 (mm^2)	408.70 ± 24.77a	424.58 ± 26.01a	259.56 ± 11.32a
Periods with BAI of ND trees > D trees	1953-1987, 1991–2016	1933-1947, 2002–2016	1937-1944, 1953–1961, 1984–1987, 1991–2016

Table 3. Sapwood concentrations of non-structural carbohydrates (NSC) shown as soluble sugars (SS), starch and total NSC and measured in declining (D) and non-declining (ND) oak trees. Values are means ± SE. Different letters indicate significant differences ($p < 0.05$; Mann-Whitney tests) between vigor classes within each species.

Species	Tree type	SS (%)	Starch (%)	NSC (%)
Quercus pubescens	D	2.28 ± 0.16a	1.82 ± 0.13a	4.10 ± 0.24a
	ND	2.22 ± 0.21a	3.24 ± 0.35b	5.46 ± 0.43b
Quercus cerris	D	2.03 ± 0.12b	2.05 ± 0.23a	4.08 ± 0.27a
	ND	1.62 ± 0.11a	2.89 ± 0.34b	4.51 ± 0.29a
Quercus frainetto	D	2.14 ± 0.12b	3.26 ± 0.28a	5.40 ± 0.42b
	ND	1.48 ± 0.13a	2.93 ± 0.33a	4.41 ± 0.44a

Table 4. *F*-values of three-way ANOVAs calculated on xylem water isotope values (δ^2H, $\delta^{18}O$) measured in samples from declining and non-declining individuals (*Tree type*) of three oak species (*Species*). Branch position (*Position*) was also considered as an effect in the analyses. The probability of the *F* values is shown between parentheses.

Effect	δ^2H (‰)	$\delta^{18}O$ (‰)	SW-excess (‰)
Species	94.47 (< 0.001)	90.07 (< 0.001)	41.58 (<0.001)
Tree Type	0.00 (0.961)	7.28 (0.007)	2.61 (0.108)
Branch Position	0.34 (0.563)	0.23 (0.633)	0.10 (0.751)
Species × Type	4.73 (0.010)	6.28 (0.002)	0.90 (0.409)
Species × Position	0.35 (0.702)	0.29 (0.748)	0.22 (0.799)
Type × Position	0.21 (0.651)	0.05 (0.812)	0.50 (0.480)
Species × Type × Position	0.94 (0.395)	0.36 (0.659)	0.85 (0.429)

Figure legends

Figure 1. Mean Palmer Drought Severity Index (PDSI) of the summer season (June to August; black bars, unitless) and mean annual temperature (red line) for the period of 1950-2017. Negative and positive PDSI values indicate dry and wet conditions, respectively.

Figure 2. Mean series of radial growth (expressed as basal area increment) from 1900 to 2016 considering declining and non-declining trees of the three study oak species: (a) *Quercus cerris*, (b) *Quercus frainetto*, and (c) *Quercus pubescens*.

Figure 3. Box-plots at the species level of (a) gravimetric soil water content (GWC) depending on the sampled soil layer (top or bottom soil) and (b) SW-excess depending on tree type (declining or non-declining). Box size represents the interquartile range, the black line is the median, the whiskers indicate variability outside the upper and lower quartiles, and individual points are outliers. In the case of GWC, only the interquartile range is depicted due to low sampling size.

Figure 4. Mean values (±SE) of (a) oxygen ($\delta^{18}O$) and (b) hydrogen ($\delta^{2}H$) isotopic compositions of xylem water in declining (D) and non-declining (ND) trees of the three studied oak species.

Figure 5. *Top panels*. Water isotope values ($\delta^{18}O$ and $\delta^{2}H$) of individual soil samples of oak stands (a, *Quercus pubescens*; b, *Quercus cerris*; c, *Quercus frainetto*). Soil water isotopes are included in the panels as follows: 0-15 cm depth (dark brown circles), 15-

30 cm (sandy brown circles), and source-based (springs, wells) groundwater estimates (blue circles). The slope (*b*) and goodness-of-fit (R^2) of the isotopic soil water line at the stand level (solid black lines) are included in the panels. *Bottom panels*. Xylem water isotope values ($\delta^{18}O$ and $\delta^{2}H$) of non-declining (green, filled circles) and declining trees (empty circles) of oak species (d, *Quercus pubescens*; e, *Quercus cerris*; f, *Quercus frainetto*). Mean values of soil water isotopes are included in the panels as follows (means ± SE): 0-15 cm depth (dark brown circles), 15-30 cm (sandy brown circles), source-based groundwater estimates (blue circles), and precipitation-based groundwater estimates (black squares). The solid black, dashed blue and dotted black lines indicate the isotopic soil water line, the local meteoric water line (LMWL), and the global meteoric water line (GMWL) respectively. The LMWL shows the linear variation of the isotopic composition of precipitation events in the study area.

Figures

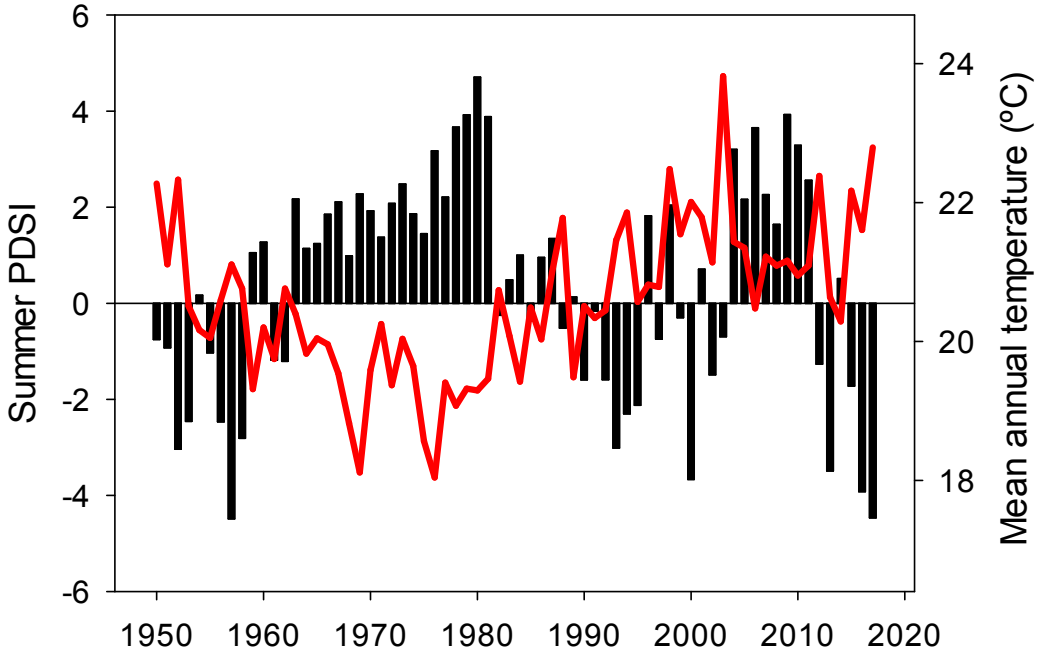

Figure 1

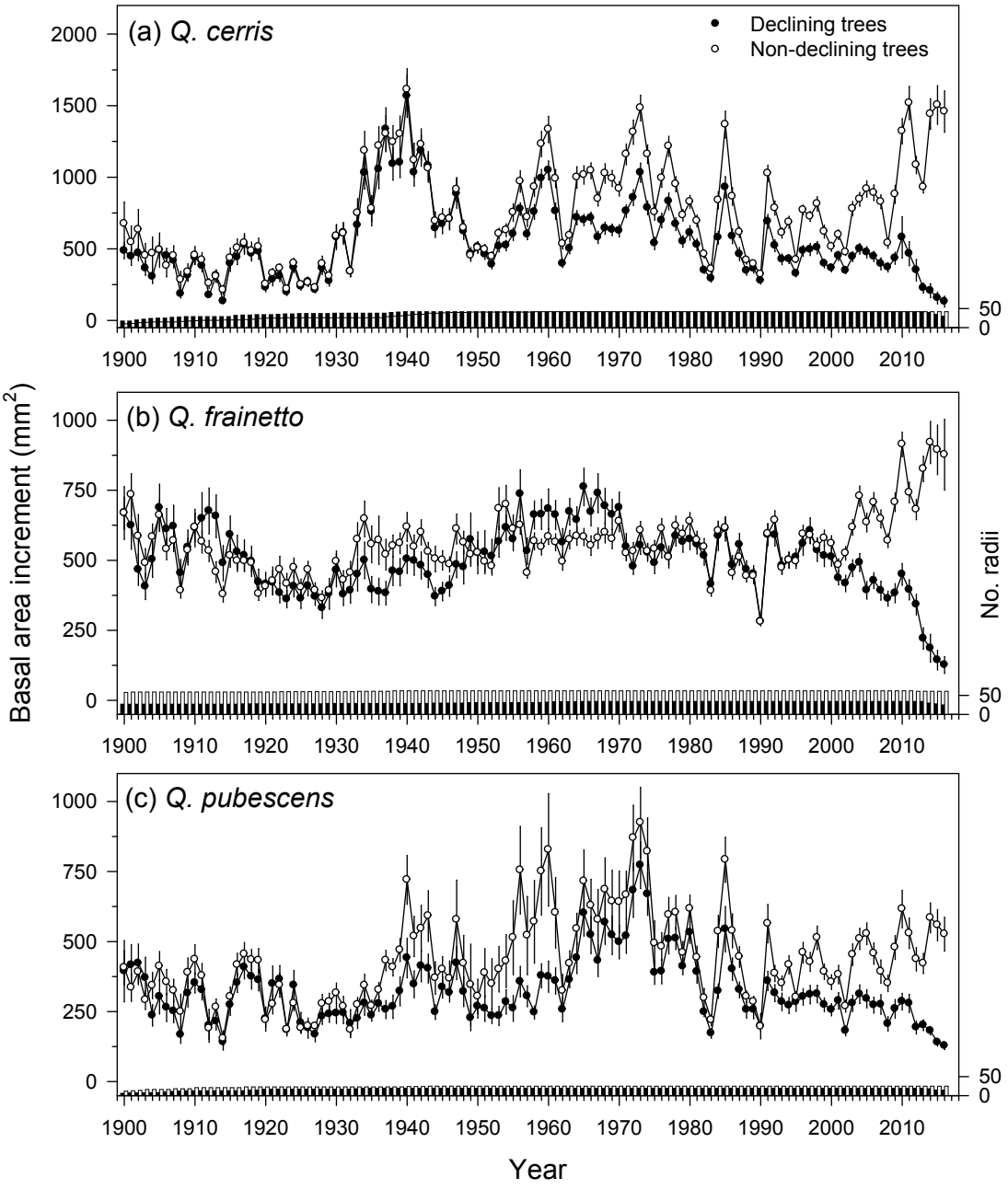
(a) Q. cerris
Declining trees
Non-declining trees
(b) Q. frainetto
(c) Q. pubescens
Basal area increment (mm2)
No. radii
Year

Figure 2

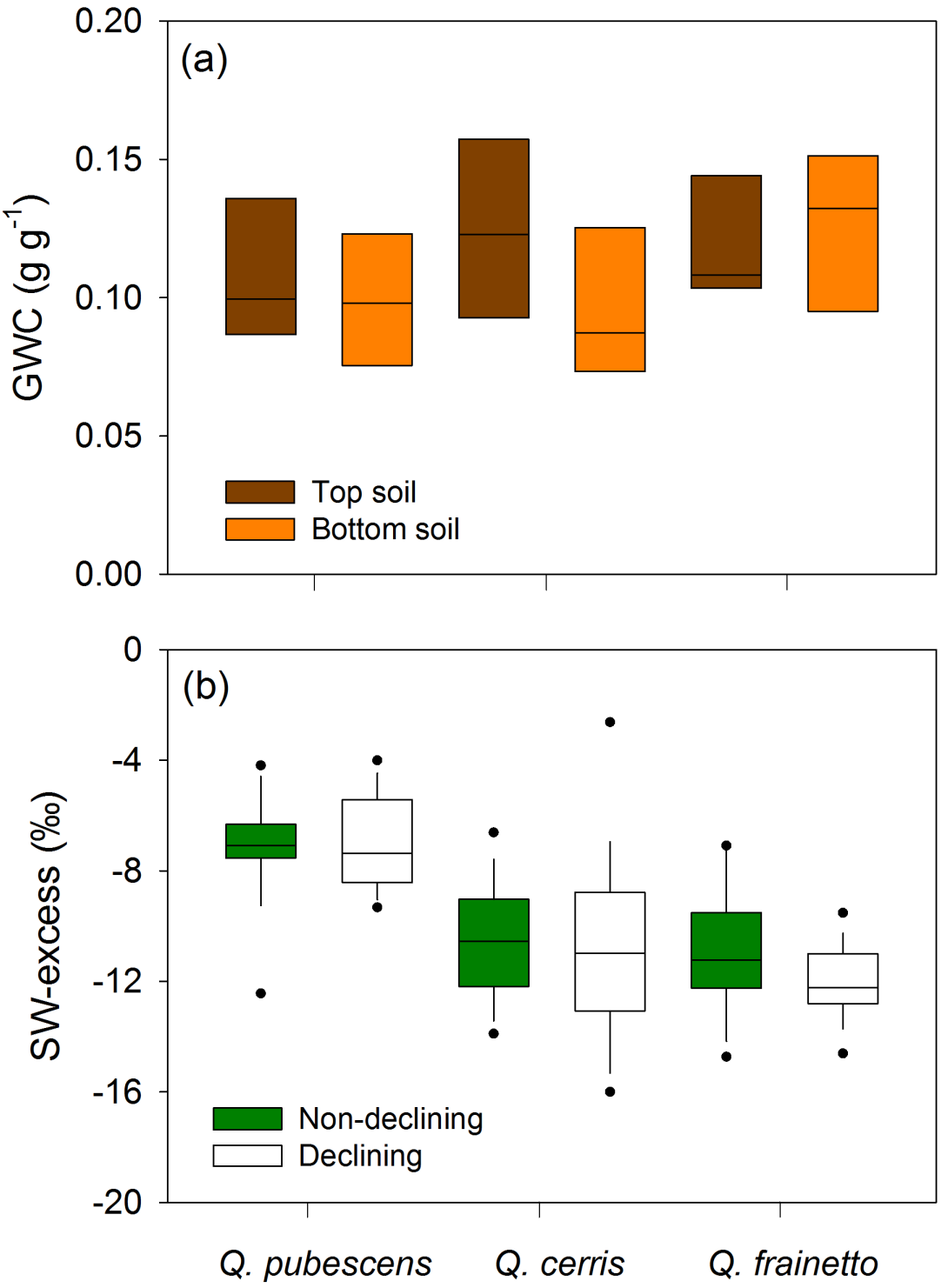
(a)
GWC (g g-1)
0.20
0.15
0.10
0.05
0.00
Top soil
Bottom soil
(b)
SW-excess (‰)
0
-4
-8
-12
-16
-20
Non-declining
Declining
Q. pubescens
Q. cerris
Q. frainetto

Figure 3

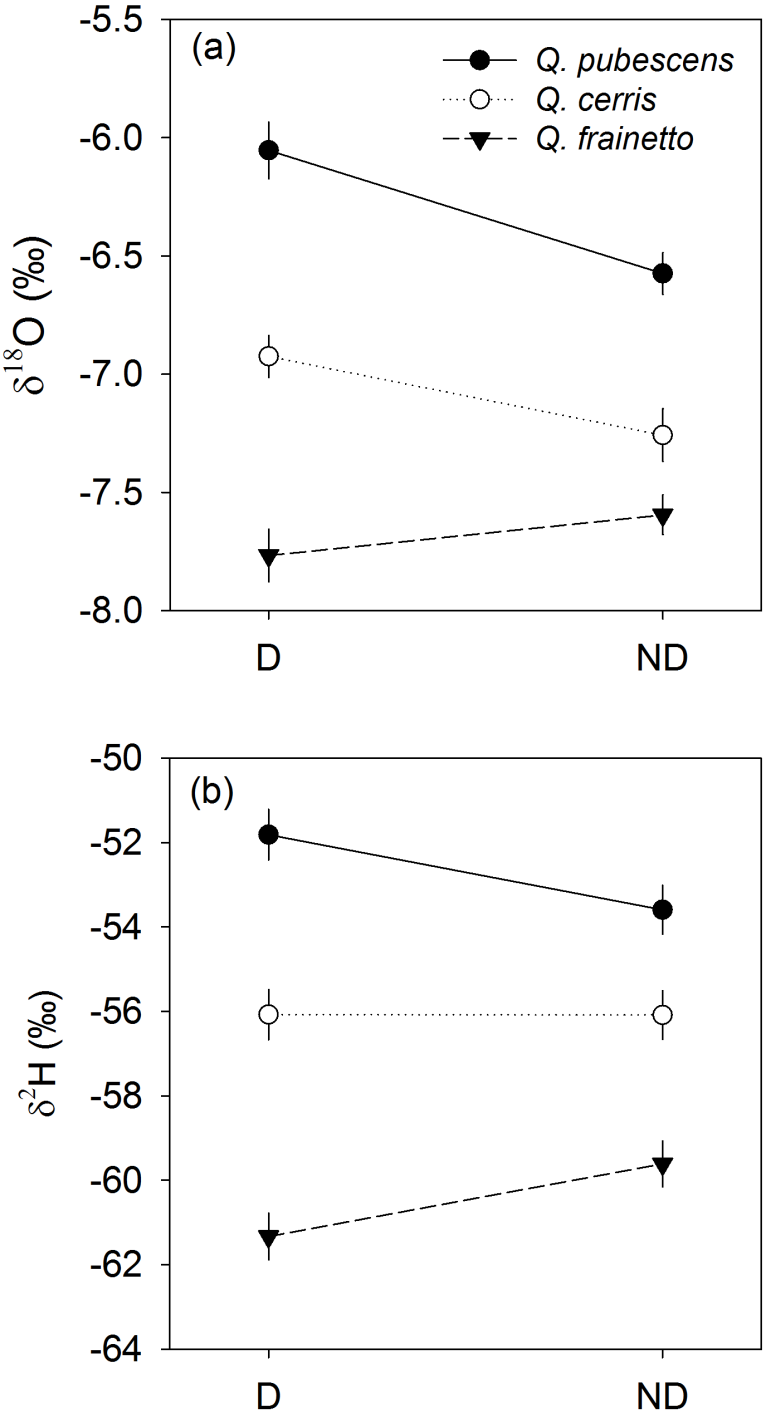
(a)
Q. pubescens
Q. cerris
Q. frainetto
-5.5
-6.0
-6.5
-7.0
-7.5
-8.0
δ18O (‰)
D
ND
(b)
-50
-52
-54
-56
-58
-60
-62
-64
δ2H (‰)
D
ND

Figure 4

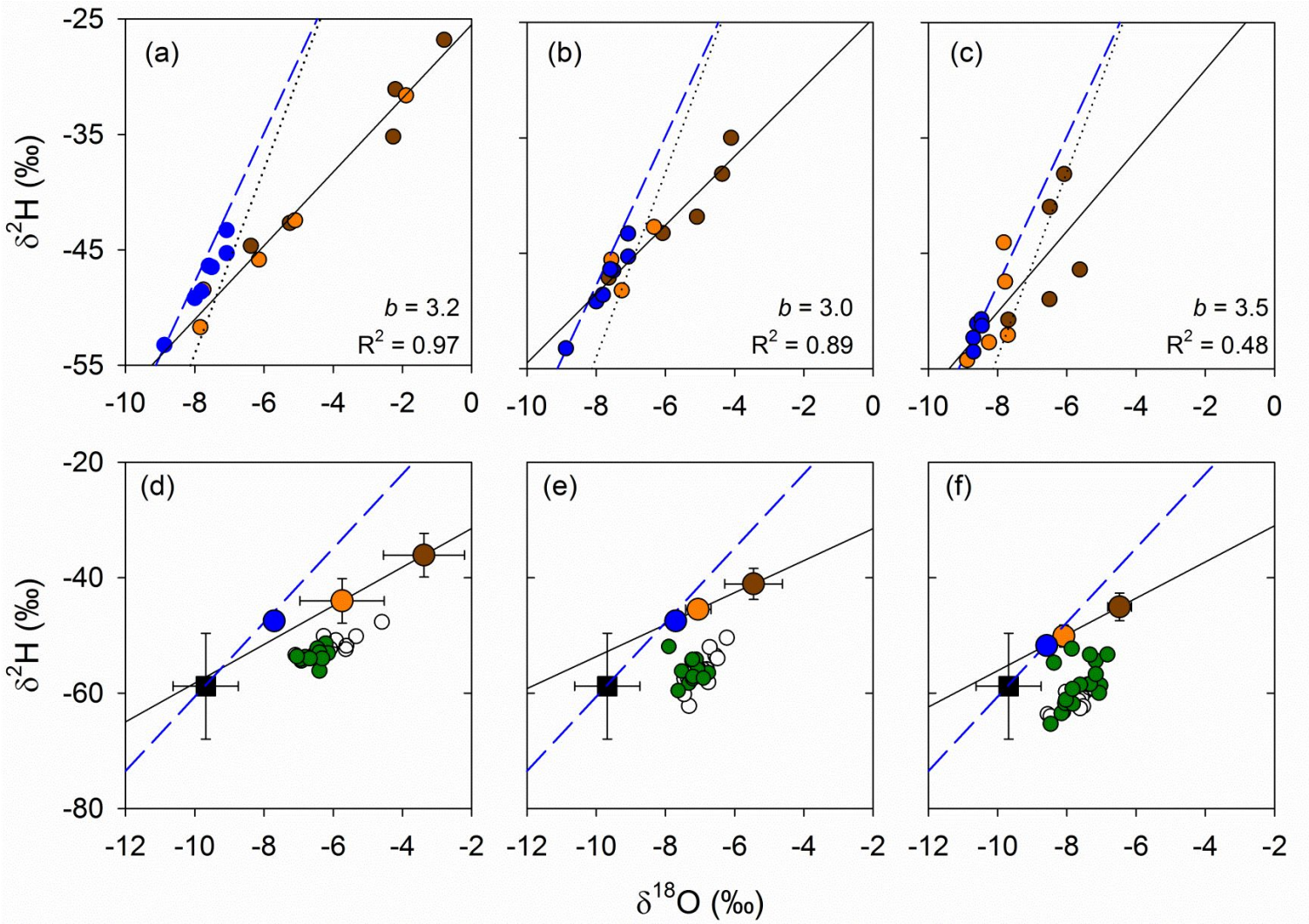

960

961 **Figure 5**

Variation in the access to deep soil water pools explains tree-to-tree differences in drought-triggered dieback of Mediterranean oaks

Francesco Ripullone[1]*, J. Julio Camarero[2], Michele Colangelo[1,2], Jordi Voltas[3,4]

[1]School of Agricultural, Forest, Food and Environmental Sciences, Univ. Basilicata, Potenza I-85100, Italy. E-mails: francesco.ripullone@unibas.it; michelecolangelo3@gmail.com

[2]Instituto Pirenaico de Ecología (IPE-CSIC), Avda. Montañana 1005, Zaragoza E-50059, Spain. E-mail: jjcamarero@ipe.csic.es

[3]Joint Research Unit CTFC - AGROTECNIO, Av. Alcalde Rovira Roure 191, 25198 Lleida, Spain.

[4]Department of Crop and Forest Sciences, Universitat de Lleida, Av. Alcalde Rovira Roure 191, 25198 Lleida, Spain. E-mail: jvoltas@pvcf.udl.cat

*Corresponding author:

Francesco Ripullone
[1]School of Agricultural, Forest,
Food and Environmental Sciences
University of Basilicata
Potenza, 85100 Italy
E-mail: francesco.ripullone@unibas.it

Key words: die-off, drought stress, Quercus, soil water sources, water isotopes.

Summary

Individual differences in the access to deep soil water pools may explain the differential damage among coexisting, conspecific trees as a consequence of drought-induced dieback. We addressed this issue by comparing the responses to a severe drought of three Mediterranean oak species with different drought tolerance: *Quercus pubescens* and *Quercus frainetto*, mainly thriving at xeric and mesic sites respectively, and *Quercus cerris*, which dominates at intermediate sites. For each species we compared coexisting declining (D) and non-declining (ND) trees. The stable isotope composition (δ^2H, $\delta^{18}O$) of xylem and soil water was used to infer a differential use of soil water sources. We also measured tree size and radial growth to quantify the long-term divergence of wood production between D and ND trees, and non-structural carbohydrates (NSC) in sapwood to evaluate if D trees presented lower NSC values. ND trees had access to deeper soil water than D trees except in *Q. frainetto*, as indicated by significantly more depleted xylem water values. However, a strong δ^2H offset between soil and xylem water isotopes observed in peak summer could suggest that both tree types were not physiologically active under extreme drought conditions. Alternative processes causing deuterium fractionation, however, could not be ruled out. Tree height and recent (last 15-25 years) growth rates in all species studied were lower in D than in ND trees by 22% and 44%, respectively. Lastly, there was not a consistent pattern on NSC sapwood concentration, showing that in *Q. pubescens* was higher in ND trees, while in *Q. frainetto* the D trees were the ones exhibiting the higher NSC concentration. We conclude that the vulnerability to drought among conspecific Mediterranean oaks depends on the differential access to deep soil water pools, which may be related to differences in rooting depth, tree size and growth rate.

Introduction

Drought-induced dieback is a global phenomenon affecting all forest biomes (Allen et al. 2015). However, neither all tree species in a community nor all tree individuals in a population are similarly affected by drought. Several studies have evidenced a diverse vulnerability to drought damage among coexisting individuals of different or the same species as a function of site features (dryness, drought intensity) or tree structural (e.g. height), hydraulic (e.g. conduit size, loss of hydraulic conductivity, hydraulic conductance) and functional characteristics (e.g., deciduousness, leaf size and density, sapwood density, root depth, gas exchange rates) (Adams et al. 2017, Greenwood et al. 2017, Martin-StPaul et al. 2017, Choat et al. 2018, Johnson et al. 2018, Olson et al. 2018, Liu et al. 2019). These studies have attempted to link such features to the major mechanisms underlying forest dieback, namely hydraulic failure and carbon starvation (McDowell et al. 2008).

Measures of drought damage such as growth decline, leaf shedding, canopy dieback or high mortality rates have been associated to traits as xylem vulnerability to cavitation or low wood density (Nardini et al. 2013). Tree species with dense wood and low specific leaf area tend to show lower post-drought mortality rates than species with the reverse characteristics (Greenwood et al. 2017). Hydraulic traits account for part of the variability in drought vulnerability across tree species, despite their potentially different importance for angiosperms and gymnosperms (Anderegg et al. 2016). For instance, tall gymnosperms are forecasted to be more prone to die due to water shortage than short-stature, hydraulically more efficient angiosperms (McDowell and Allen 2015). A similar reasoning has been applied at the community level in a way that the

diversity in species hydraulic traits in temperate and boreal forests explained part of the ecosystem carbon fluxes after a drought (Anderegg et al. 2018). Yet within a particular forest, predicting which tree species and individuals are most likely to die or survive after a severe drought remains a challenge. Individual tree predispositions due to either differential plastic responses or constitutive genetic differences for functional traits related to drought resistance could buffer damage due to drought stress (Voltas et al. 2013).

At stand level, variability in traits related to drought resistance is expected to show a wider range between than within species. Therefore, understanding and quantifying the vulnerability to drought within a species is a first step towards predicting the probability of individual survival. Growth trends (tree-ring-width data) have been related to crown dieback and used as early-warning signals to identify and characterize declining and, therefore, more vulnerable individuals within a species (Camarero et al. 2015). However, this approach seems feasible in some species, for instance in some conifers whose susceptible individuals show long periods (>20 yrs.) of growth decline, but not in others as oaks which show shorter periods (5-20 yrs.) of growth reduction (Cailleret et al. 2018). This may be due to the fact that oaks display an anisohydric behavior with pronounced declines in leaf midday water potential during drought and may be prone to xylem cavitation and hydraulic failure, whereas isohydric conifers rapidly close stomata as vapor pressure deficit (VPD) rises (Klein 2014). In the case of ring-porous Mediterranean oak species, hotter droughts may enhance atmospheric evaporative demand shifting VPD towards a critical threshold, surpassing their limit of hydraulic safety (Tognetti et al. 1998, Colangelo et al. 2017a). Consequently, hydraulic failure could be a plausible mechanism of drought-induced dieback in Mediterranean oaks.

Drought-tolerance mechanisms are diverse and not restricted to resistance to xylem cavitation, stomatal control of water use or increased carbon storage (Pinheiro et al. 2005). These mechanisms also include different access to soil water pools, with shallow- and deep-rooted species often showing high and low drought damage levels, respectively (Padilla and Puignaire 2007, Hasselquist et al. 2010, Pivovaroff et al. 2016, Antunes et al. 2018, Chitra-Tarak et al. 2018). Drought stress often acts as a major driver of dieback, usually linked to site-specific soil conditions, such as the characteristics of soil parent material that inhibits root development or access to groundwater (Costa et al. 2010). Indeed, large belowground losses of hydraulic conductance and shallow rooting depths are often associated with species that exhibit greater mortality after severe droughts (Johnson et al. 2018). According to stable isotope evidence, roots may take up deep soil water during dry periods which allow trees to buffer drought effects (Ehleringer and Dawson1992, Barbeta and Peñuelas, 2017). Coexisting species may show different water isotopic signals corresponding to contrasting – and highly dynamic – water-use strategies during drought as observed in Mediterranean forests (Moreno-Gutierrez et al. 2012, Del Castillo et al. 2016, Dubbert et al. 2019, Dubbert and Werner 2019). However, tree species may tap increasingly deep sources of soil water as drought intensifies (Meinzer et al. 1999, Voltas et al. 2015). The access to deep water reservoirs could buffer the predicted negative impacts of hotter droughts on forests (Sánchez-Salguero et al. 2017) and allow trees to survive and recover in hydrologic refugia where groundwater is available throughout the year (McLaughlin et al. 2017).

Here we test the idea that tree-to-tree differences in the use of deep soil water may explain the differential damage of coexisting, conspecific oak individuals due to drought-induced dieback. For this purpose, we use information of the stable isotope

composition ($\delta^{18}O$ and $\delta^{2}H$) of soil and xylem water obtained at the peak of summer drought. We also quantify changes in radial growth and in the sapwood concentration of non-structural carbohydrates (NSC) of conspecific trees showing different vulnerability to drought. We expect that non-declining, asymptomatic trees will be able to extract water from deeper soil water pools than declining, symptomatic trees. We also expect this difference to be magnified in the species occupying the most xeric sites (*Q. pubescens*), subjected to frequent and intense episodes of water shortage, compared with the species typical of mesic sites (*Q. frainetto*), which grows more, depends on shallower soil water and has a lower root-to-shoot ratio (Ledo et al. 2018). Lastly, we hypothesize that declining trees will show a lower sapwood NSC concentration than non-declining trees.

Materials and methods

Study sites

We studied three Mediterranean, deciduous, ring-porous oak species in southern Italy: two species (*Quercus pubescens* L., *Quercus cerris* L.) were sampled in different stands located at the Gorgoglione municipality (40° 21' 51'' N, 16° 10' 34''E, 825 m a.s.l.), and the third species (*Quercus frainetto* Ten.) was sampled in a stand near San Paolo Albanese (40° 01' 20'' N, 16° 20' 46'' E, 950 m a.s.l.). *Q. pubescens* is widely distributed across southern Europe, *Q. cerris* is found in the Italian and Balkan Peninsulas, Asia Minor, central Europe and France, and *Q. frainetto* is found across the Western Mediterranean Basin (San-Miguel-Ayanz et al. 2016). These species often coexist (and hybridize) in sites with mean annual temperature (MAT) of 6-18 ºC and annual precipitation (MAP) of 500-1300 mm. In the study areas climate is Mediterranean, characterised by dry and warm summers that have become particularly

noticeable during the last decade (Fig. 1). At San Paolo Albanese, total June to August precipitation is 79 mm and winters are wet and mild. At this site, MAT is 16.4 °C and MAP is 742 mm (data from Oriolo station, 40° 03'11''N, 16° 26' 47'' E, 445 m a.s.l., 1950–2016 period). At Gorgoglione, total June to August precipitation is 93 mm and winters are wet and mild. At this site, MAT is 14.6 °C and MAP is 722 mm (data from Gorgoglione station, 40' 240'' N, 16' 090'' E, 796 m, 1950–2016 period). In both sites drought occurs from June to August.

To assess long-term climate trends we used the E-OBS 0.25º-gridded climate dataset considering the 1950-2017 period (Cornes et al. 2018). We downloaded annual and monthly temperature and precipitation data for the grid with coordinates 16.00-16.25º W and 40.00-40.25º N using the climate explorer webpage (https://climexp.knmi.nl). We also estimated drought severity using the self-calibrating Palmer Drought Severity Index (hereafter PDSI) based on the gridded monthly precipitation and temperature data (Wells et al. 2004). We calculated the summer PDSI (from June to August) to quantify summer drought severity.

Soils are sandy-loam textured with a mean pH of 7.5 and mostly shallow (i.e. ranging from 0.2 to 0.6 m depth). They rest on a soft sedimentary fractured bedrock consisting of an alternation of sandstones, pelites and conglomerates layers (Gorgoglione Flysch Formation), which typify part of the Apennines chain.

In the study area, the three species coexist but *Q. pubescens* preferentially occupies the most xeric sites (e.g., steep slopes with southern aspect and shallow soils), *Q. frainetto* is found in mesic sites (e.g., gentle slopes with northern aspect and relatively deep soils), and *Q. cerris* abounds in intermediate locations (Gentilesca et al. 2017). In San Paolo Albanese, the vegetation is formed by a pure high forest of *Q. frainetto* for a density of 348 trees ha^{-1}, whilst in Gorgoglione the stand is a mixed high

forest with a mean density of 600 trees ha^{-1} dominated by *Quercus cerris* L. (71%), followed by *Quercus pubescens* L. (25%) and other broadleaf species (4%). These oak forests were formerly managed as coppices with livestock grazing.

All species have shown symptoms corresponding to drought-induced dieback since the turn of this century, specifically canopy dieback, leaf loss and withering, growth decline, and high mortality (Colangelo et al. 2017a, 2017b). In the most affected stands, more than 50% of mature specimens showed dieback symptoms and 15% recently died (Colangelo et al. 2018).

Field sampling

To characterize stand structure (density, basal area) and assess the degree of dieback damage we followed a similar procedure as in Colangelo et al. (2017a). Seven circular plots (radius of 15 m) were randomly located in each site and in areas where each species was dominant. Within each plot, dieback of all mature oak trees was characterized by a visual assessment of crown transparency made by two independent observations of the same tree (Camarero et al. 2016). Declining oaks (hereafter D trees) were considered those with crown transparency higher than 50%, whereas non-declining oaks (hereafter ND trees) were considered those with transparency lower than 50%. The size (diameter at 1.3 m, total height) of all trees was measured.

Radial growth

For each species, we selected 12-21 paired trees of different vigour, i.e. neighbouring ND and D oaks located 10–15 m apart at maximum. They were sampled in late summer of 2016 to quantify their radial-growth trends using dendrochronology. Two cores were

sampled at breast height (1.30 m) from each tree at opposite directions and perpendicular to the maximum slope using a 5-mm Pressler increment borer.

The transversal surface of cores was cut using a sledge microtome to differentiate the annual tree rings (Gärtner and Nievergelt 2010). Rings were visually cross-dated and measured with precision of 0.01 mm using a binocular microscope coupled to a computer with the LINTAB package (Rinntech, Heidelberg, Germany). The COFECHA program (Holmes 1983) was used to evaluate the visual cross-dating of tree-ring width data. To quantify growth trends and to partially avoid the age- / size-related decrease in tree-ring width, we transformed these data into annual basal area increment (BAI) assuming a circular shape of stems. Tree age at 1.3 m was estimated from increment cores that either included the pith or were close to it (the arc of the innermost rings was visible). In the second case, we followed Duncan (1989) and fitted a template of concentric circles to the curve of the innermost rings to estimate the number of missing rings.

Soil and xylem water sampling and extraction, groundwater collection and isotopic analyses

The soil and stem xylem sampling took place in August 2017 during an exceptionally hot and dry period, with a monthly temperature over 2 ºC higher and precipitation about 40 mm lower than long-term averages for the region (22.8 °C and 56 mm). This resulted in the most severe drought occurring over the last 70 years (Fig. 1). Information on the use of soil water sources for each species and tree type (D, ND) was obtained using measurements of water isotope ratios (oxygen and hydrogen isotope composition, $\delta^{18}O$ and $\delta^{2}H$) for different soil depths as well as for xylem water (Martín-Gómez et al. 2015, Grossiord et al. 2017).

Xylem samples were obtained from 11:00 to 13:00 h solar time from twelve D and twelve ND trees per species at Gorgoglione (August 23rd) and San Paolo Albanese (August 24th). Two branches were sampled from the upper third crown of each tree at north- and south-facing sides using telescopic loppers. Sampled branches were *ca.* 1.5-3.0 cm thick and shoot segments (5-7 cm long) were cut and then bark-peeled, placed immediately into glass vials and frozen in dry ice to avoid evaporation. Soil samples were collected for the same days at two depths (0–15 cm and ≈15–40 cm, that is, until reaching the bedrock) using a straight tube probe carefully cleaned between consecutive samplings. From 07:00 to 09:00 h solar time, samples were taken from soil pits located at intermediate positions between pairs of sampled D and ND individuals for each species. The soil extracted was placed rapidly into glass vials and frozen in dry ice. All samples were kept frozen until processing and analysis.

Xylem and soil water was extracted by cryogenic vacuum distillation (Martín-Gómez et al. 2015). Sample tubes were placed in a heated silicone oil bath (110–120°C), and connected with Ultra-Torr unions (Swagelok Co., Solon, OH, USA) to a vacuum system for a constant vacuum pressure of *ca.* 10^{-2} mbar, including U-shaped water traps in series that were refrigerated with liquid N_2. The extraction time was 90 min for xylem and 120 min for soil samples. Using exactly the same extraction device, this extraction time has been previously shown to be enough to extract all available water from similar soil and xylem samples (i.e., involving sub-mediterranean oaks) to those of our study (Martín-Gómez et al. 2017). Captured water was then transferred into cap-crimp 2-ml vials, and stored at 4°C until analysis. Gravimetric soil water content (GWC) was assessed for each sample using the sample weight before and after water extraction. A subset of representative samples, including both xylem and soil samples, was checked for complete water extraction by oven drying them at 105 °C for 36 h and

reweighing them. In all cases, the samples did not show a significant weight loss when placed in the drying oven.

The oxygen and hydrogen isotopic composition ($\delta^{18}O$ and $\delta^{2}H$, respectively) of water was determined by isotope ratio infrared spectroscopy (IRIS) using a Picarro L2120-i coupled to an A0211 high-precision vaporizer (Picarro Inc., Sunnyvale, CA, USA). The estimated precision, based on the repeated analysis of four reference water samples, was 0.10‰ for $\delta^{18}O$ and 0.40‰ for $\delta^{2}H$. Residual organic contaminants in the distilled water can hamper the interpretation of plant and soil water isotopic composition conducted with IRIS (Martín-Gómez et al., 2015). The occurrence of contaminants was tested using Picarro's CHEMCORRECT post-processing software and corrected, when necessary, following Martín-Gómez et al. (2015).

The local meteoric water line (LMWL) was obtained from rainfall isotope data collected in the Mt. Vulture volcano (40º 57' N, 15º 38' E), southern Italy, for the period 2002-2004 (Paternoster et al. 2008). LMWL was described as $\delta^{2}H = 3.72 + 6.44 \times \delta^{18}O$ (R^2=0.99). For groundwater, two alternative estimates were used: the weighted average of monthly isotopic signatures of precipitation from October to April (considered as the soil recharge period in the Mediterranean) at Mt. Vulture (within a 80-km radius from the experimental sites) over the same period using an available dataset built about 15 year ago (method 1), and the average of samples of water collected from seven (Gorgoglione) or five (San Paolo Albanese) nearby fountains or wells located within a 5-km radius of the sampled stands (method 2). These water samples were obtained at the end of June 2019. The results were as follows: -9.6 ± 0.94‰ (mean ± standard deviation) and -58.8 ± 9.17‰ (method 1), -7.7 ± 0.23‰ and -47.5 ± 1.21‰ (method 2, Gorgoglione), and -8.5 ± 0.17‰ and -51.8 ± 0.84‰ (method 2, San Paolo Albanese) for $\delta^{18}O$ and $\delta^{2}H$, respectively. The estimates of method 2 could

be influenced by the different origins of groundwater, either wells or fountains, the latter being prone to evaporative enrichment if water is openly exposed. A test for differences between the inferred isotopic compositions of groundwater depending on their origin (well or fountain) did not reveal a significant evaporative enrichment in samples originating from fountains (results not shown), which led us to use both water sources for groundwater estimation.

Evaporative enrichment of xylem water, which has a disproportionately greater effect on $\delta^{18}O$ than on $\delta^{2}H$ (Craig, 1961), was quantified through the concept of the soil water line-conditioned excess (SW-excess), as proposed by Barbeta et al. (2019). The SW-excess describes the potential offset of xylem water samples relative to their soil water line, and represents a modification of the line-conditioned excess (Landwehr and Coplen 2006), which in turn describes an offset of water samples relative to the LMWL. The SW-excess was computed as:

$$\text{SW-excess} = \delta^{2}H - a_S\delta^{18}O - b_S \quad [1]$$

where a_S and b_S are the slope and intercept, respectively, of the soil water line for a particular site and species, and $\delta^{2}H$ and $\delta^{18}O$ correspond to the isotopic composition of a xylem water sample collected on that site and species. The slope and intercept a_S and b_S were computed by performing a linear regression on all the soil water isotope data from the top and bottom horizons collected per site and species. The SW-excess has been recently used to quantify hydrogen isotope offsets occurring when $\delta^{2}H$ of xylem water is more depleted than the considered water sources (Barbeta et al. 2019), but its application is restricted to monotonic soil isotopic profiles. Negative SW-excess values indicate xylem samples that are more depleted in deuterium than the soil water line and are, thus, positioned below soil water samples in a $\delta^{18}O$ - $\delta^{2}H$ plot.

Non-structural carbohydrates (NSC) in sapwood

To assess the carbon status of coexisting ND and D trees we quantified sapwood NSC concentrations. We selected five trees per vigour class and sampled their sapwood at 1.3 m using Pressler increment borers (see Colangelo et al. 2017a). The sapwood was visually distinguished in the field and separated using a razor blade. Sapwood samples were collected in summer 2018, transported in a portable cooler to the laboratory, and stored at −20 °C until freeze-dried. Then, they were weighed and milled to a homogeneous powder in a ball mill (Retsch Mixer MM301, Leeds, UK). Soluble sugars were extracted with 80% (v/v) ethanol and their concentration was colorimetrically determined using the phenol-sulfuric method (Buysse and Merckx 1993). Starch and complex sugars remaining after ethanol extraction were enzymatically digested as described in Colangelo et al. (2017a). NSCs measured after ethanol extractions are referred to as soluble sugars (SS), and NSCs after enzymatic digestion are referred to as starch. Total NSC concentration (% dry matter) was calculated as the sum of SS and starch concentrations.

Statistical analyses

To compare variables between ND and D trees of each species (tree density, diameter at 1.3 m, height, age at 1.3 m, BAI, NSCs) and between soil depths (gravimetric soil water content) we used the Mann-Whitney *U* test. We tested if BAI of ND and D trees differed using the Wilcoxon rank-sum test because this statistic is robust against deviations from normality and autocorrelation (Hentschel et al. 2014).

For soil isotope records ($\delta^{18}O$ and $\delta^{2}H$), we fitted a two-way analysis of variance (ANOVA) considering sampled stand (*Q. cerris*, *Q. frainetto*, *Q. pubescens*) and soil depth (top, bottom) as main factors. For each sampled stand, we also fitted a

heterogeneity of slopes ANOVA to detect differences in the relative response of $\delta^{18}O$ to changes in $\delta^{2}H$ according to soil depth. To this end, the variability of $\delta^{18}O$ values was explained by soil depth, and $\delta^{2}H$ was introduced as covariable together with its interaction with soil depth.

For xylem isotope values ($\delta^{18}O$, $\delta^{2}H$ and SW-excess), we used a three-way ANOVA considering the following fixed factors and their interactions: species (*Q. cerris*, *Q. frainetto*, *Q. pubescens*), tree type (D, ND), and branch position (north, south). In addition, we allowed for heterogeneous residual variances at the tree type level. The better fit of this model compared with a model having homogeneous residuals was checked with AIC and BIC statistics. Mixed model ANOVAs were performed using the MIXED procedure of SAS/STAT v.9.4 (SAS Institute Inc., Cary, NC, USA).

Results

Tree size and radial growth

D and ND trees presented similar diameter and age irrespective of the oak species, but ND trees were significantly taller ($p<0.05$) than conspecific D trees, with differences ranging from 23% (*Q. cerris*) to 32% (*Q. frainetto* and *Q. pubescens*). These differences were not clearly related to stand density (Table 1). However, the density of D trees was significantly higher than that of ND trees in the case of *Q. cerris* and *Q. frainetto*.

The mean growth rate (BAI) of the last 25 years (period 1991-2016) was significantly higher in ND than in D trees for all species (Table 2). The relative growth reductions (BAI difference between ND and D trees) were 53.7%, 35.2 % and 42.0% in *Q. cerris*, *Q. frainetto* and *Q. pubescens*, respectively. For all oak species, ND trees grew more than D trees from 2002 to 2016, but this difference was also significant in

other previous periods, depending on each species (Table 2). Severe BAI reductions were observed in 1952, 1957, 1962, 1967, 1970, 1975, 1982-1983, 1990, 1995, 2002, and 2013 (Fig. 2). The recent divergence in growth between ND and D trees started in 2002 in the case of *Q. frainetto*, but higher growth rates in ND than in D trees could be traced back to 1953 in the other two species (Fig. 2, Table 2).

Differences in NSC between tree types

We found a significantly lower sapwood SS concentration in ND than in D trees of *Q. cerris* and *Q. frainetto*, but a higher starch concentration in ND trees of *Q. cerris* and *Q. pubescens* (Table 3). Total NSC concentration was lower in D trees of *Q. pubescens*, but higher in *Q. frainetto* D trees, with non-significant differences observed for *Q. cerris*.

Soil and xylem water isotopes

Top soil water was significantly more enriched than bottom soil water for both isotopes (p = 0.006 and 0.014 for $\delta^{18}O$ and $\delta^{2}H$, respectively) irrespective of sampled stand, denoting evaporative enrichment at the soil surface. There were also differences among stands for both isotopes ($p < 0.05$), with soil water of the *Q. pubescens* stand being significantly more enriched than that of *Q. frainetto*, hence suggesting higher soil evaporative enrichment for *Q. pubescens*, followed by *Q. cerris* and *Q. frainetto.* Except in very few cases, the soil water samples were consistently placed on the right side of the LMWL line, regardless of the sampled stand (Fig. 5, top panels).

The heterogeneity of slopes ANOVA did not detect differential soil evaporative enrichment as dependent on soil depth layer (i.e., different slopes conditional to soil depth), which indicated monotonic isotopic soil profiles across stands (slopes ranging

between 3.0 and 3.5; Fig. 5, top panels). These monotonic soil profiles may be related to the relatively shallow soils typical of these ecosystems. Consequently, direct evaporation may have exerted a similar effect across soil depths.

These soil slope values were significantly smaller than the slope of the LMWL line (6.4). The GWC did not significantly differ between soil depths for each sampled stand, with mean values of 10.4%, 11.1% and 12.2% for *Q. pubescens*, *Q. cerris* and *Q. frainetto*, respectively (Fig. 3a). Since soil physicochemical properties were approximately homogeneous across soil depths (e.g. pH = 7.6 ± 0.1 and 7.5 ± 0.2, EC = 182 ± 17 and 185 ± 37 µS cm^{-1} for top and bottom soil, respectively, at Gorgoglione), we estimated, based on the water retention properties of sandy loam soils, that the permanent wilting point was reached for roughly 30% of soil samples by end August. Top soil GWC was negatively correlated with soil water $\delta^{18}O$ across stands (r = -0.62; p = 0.01) but not with $\delta^{2}H$ (r= -0.42; p = 0.11). On the other hand, bottom soil GWC was unrelated to either $\delta^{18}O$ (r= -0.01; $p > 0.05$) or $\delta^{2}H$ (r= +0.17; $p > 0.05$).

For xylem isotopic composition, significant differences were observed among species for $\delta^{18}O$ and $\delta^{2}H$, and between tree types for $\delta^{18}O$ only (Table 4). However, there was a significant interaction between species and tree type for both isotopes. Declining trees of *Q. pubescens* and *Q. cerris* showed significantly higher $\delta^{18}O$ values than ND trees, whereas both tree types had statistically similar $\delta^{18}O$ values for *Q. frainetto* (Fig. 4a). Also, D trees had significantly higher $\delta^{2}H$ values than ND trees for *Q. pubescens*, although non-significant differences were found for *Q. cerris* and statistically higher $\delta^{2}H$ values of ND trees were observed for *Q. frainetto* (Fig. 4b). Despite such differences, the ranking of species was consistent across tree types, with *Q. pubescens* showing the least negative values, followed by *Q. cerris* and, finally, *Q. frainetto*. There were neither significant differences between branch positions nor

significant interactions involving this factor, suggesting lack of differential access to water sources across the tree crown.

Visual inspection of the xylem water samples in the dual-isotope space indicated that the isotopic signatures of the oak trees clearly departed from the LMWL line and, also, from the isotopic soil water evaporation lines (Fig. 5, bottom panels). In particular, xylem water samples had consistently more depleted δ^2H values than top and bottom soil layers ($p < 0.001$) for all oak species. Hence, xylem samples fell outside the range of the monitored water sources in the dual-isotope space, including groundwater estimated from natural springs (Fig. 5, bottom panels). For most sampled stands, the lower part of the isotopic soil water evaporation line crossed the LMWL line at the exact position of the natural spring-based groundwater estimate in the dual-isotope space. The exception was the *Q. pubescens* stand, in which the isotopic soil water evaporation line crossed the LMWL line close to the position of the precipitation-based groundwater estimate.

According to soil water $\delta^{18}O$ alone, the oak trees mainly took up water from deep soil sources (bottom soil or groundwater), irrespective of oak species. This was suggested by xylem water $\delta^{18}O$ values that were intermediate between the bottom soil and the groundwater $\delta^{18}O$ values in most cases (Fig. 5, bottom panels). However, the xylem water of *Q. pubescens* and *Q. cerris* was closer to the bottom soil values (15-40 cm), especially in the case of declining trees. On the other hand, the xylem water of *Q. frainetto* took values across the range of values of the bottom soil and the groundwater but closer to groundwater, without obvious differences between D and ND trees.

The isotopic offset between xylem and soil water samples was examined through calculation of the SW-excess. Overall, the SW-excess was significantly larger in *Q. cerris* (SW-excess = -10.27 ± 3.5; mean ± SD) and *Q. frainetto* (-11.89 ± 1.6) compared

with *Q. pubescens* (-7.1 ± 1.7) (Fig. 3b), but non-significant effects of tree type and of the interaction between tree type and species were observed (Table 4). Moreover, we did not find significant effects associated with branch position or its interaction with tree type and species.

Discussion

As hypothesized, our results indicate than non-declining oak trees of *Q. cerris* and *Q. pubescens* extracted deeper soil water than declining trees during peak summer, suggesting the existence of tree-to-tree variability in root access to different soil layers. The exception to this pattern was *Q. frainetto*. For this species, D and ND conspecifics likely drew the same deep water using a similar survival strategy to that of the ND individuals in *Q. cerris* and *Q. pubescens*, despite *Q. frainetto* is mainly found in mesic Mediterranean sites with *a priori* less requirements on preferential access to deeper water. On the other hand, we did not find support for our second hypothesis stating that declining trees should show a lower total NSC concentration than non-declining trees regardless of species, which could be indicative of carbon starvation as die-back mechanism (*cf*. McDowell et al. 2008).

Mediterranean oaks can keep their physiological activity during summer by relying on water reservoirs like groundwater or deep soil layers (Del Castillo et al. 2016, Martín-Gómez et al. 2017). A strong dependence of deciduous oaks on rainfall recharge during autumn and winter has been observed in the western Mediterranean basin through the analysis of stable oxygen isotopes in wood cellulose (Shestakova et al. 2014). In this regard, the differences between declining and non-declining trees were only evident for the more xeric species, which reinforces the importance of the reliance on deep soil water pools of oaks for survival under progressively hotter droughts.

However, we observed a clear isotopic offset between soil and xylem water isotopes in peak summer regardless of the species. For this reason, we could not quantify the relative contribution of different soil depths as water sources for declining and non-declining trees using a mixing model (e.g. Voltas et al. 2015).

In fact, the xylem samples were placed along an alternative evaporation line of soil water that may correspond to previous months of the growing season, as previously reported for *Q. ilex* subjected to an acute drought (Del Castillo et al. 2016). This might indicate that both tree types were not actively taking up water in peak summer, therefore ceasing their physiological activity (i.e. transpiration) during the extreme summer drought of 2017. This is feasible taking into account that there was 0 mm of precipitation in July and August 2017, and the precipitation for the first half of the year was only 61% of a normal year. The low soil GWC also points in this direction. The analysis of seasonal dynamics of root access to different water pools would provide additional clues on the physiological performance of healthy and declining oak trees, as demonstrated for understanding differences among functional types in drought-prone environments (Barbeta et al. 2015; Martín-Gómez et al. 2017; Antunes et al. 2018).

The isotopic offset between xylem and soil water samples, however, does not necessarily indicates an older age of water kept by the trees in peak summer. Indeed, there is a growing body of literature reporting on deuterium fractionation in controlled experiments (Vargas et al. 2017) or natural conditions (Evaristo and McDonnell 2017, Barbeta et al. 2019, Oerter and Bowen 2019), either under full irrigation or drought stress. Consequently, a number of alternative but non-exclusive explanations have been raised to explain isotope offsets occurring when xylem water is more ^{2}H-depleted than the considered water sources. Amongst them, root discrimination against the heavier ^{2}H may occur in the unsaturated soil-root interface following vapour condensation, a

process becoming progressively more important as soil dries out (Vargas et al. 2017, Barbeta et al. 2019). This challenges the general assumption of lack of fractionation during root water uptake (Lin and Sternberg 1993). Also, spatial heterogeneity in the stable isotopic composition of soil water with different mobility may also impact on xylem isotopic signatures (Orlowski et al. 2018, Dubbert et al. 2019, Oerter and Bowen 2019), thereby complicating tree water source identification. Deuterium fractionation has also been reported between xylem sap and root or stem tissue water in drylands (Zhao et al. 2016), and water cycling, storage and exchange is known to be more common than previously assumed in plants, which together could change xylem isotopic composition. We can neither discard the influence of cavitation processes for anisohydric species, such as oaks, on the explanation of the offset in xylem isotopic composition. In fact, xylem water sampling took place at noon solar time during peak summer, which may have increased the risk of cavitation and hydraulic failure in the sampled trees, thereby mediating the water exchange between phloem and xylem due to embolism repair and, hence, the observed xylem offset (Nardini et al. 2011, Pfautsch et al. 2015). The rock permeability of the area, which can create differences in exchangeable water held in weathered bedrock, has been also postulated as an alternative source of water for plants that might explain isotopic offsets (Palacio et al. 2014, Oshun et al. 2015, Barbeta & Peñuelas 2017, Rempe & Dietrich 2018).

A role of mycorrhizal fungi on the preferential uptake of the light hydrogen isotope by plants has been also proposed (Poca et al. 2019), again questioning the fractionation-free assumption during root water uptake. Since free-living fungi and mycorrhizal species are negatively affected by drought (Castaño et al. 2018), the extent of root discrimination against the heavier ^{2}H is expected to be relatively more important under optimal soil water conditions. In fact, the stand most affected by drought (*Q.*

pubescens) showed a significantly higher (i.e., less negative) SW-excess, which suggests potential effects of soil fungi on tree water uptake being more important in less water-limited sites (Rempe and Dietrich 2018). Regardless of the relative magnitude of deuterium fractionation processes, the closer values of xylem water to groundwater in non-declining trees of *Q. cerris* and *Q. pubescens* point to a preferential access to deep water reservoirs for healthy individuals of these species.

Only declining trees of *Q. pubescens*, the species dominant under the most xeric conditions of our study and which better tolerates drought (Tognetti et al. 1998), presented a lower NSC concentration than non-declining trees. Conversely, *Q. cerris* trees of different vigor presented a similar total NSC concentration. In fact, starch concentration was significantly lower in declining trees of *Q. cerris*, but SS concentration was higher in declining trees of the same species. In the case of *Q. frainetto*, declining trees showed a significantly higher total NSC concentration than non-declining individuals (Colangelo et al. 2017a). In this species, declining trees, which also showed lower recent growth rates than non-declining trees, may be storing carbon not used for producing stem wood as sapwood NSCs, in agreement with previous theoretical (Tardieu et al. 2011, Körner 2013) and empirical evidences (Muller et al. 2011). These studies emphasize that carbon sinks (e.g., cambium and leaf growth) are much more sensitive to water deficit (i.e., their activity is restricted earlier or at lower levels of drought stress) than carbon sources (e.g., photosynthesis rate). Furthermore, the higher concentrations of soluble sugars in declining trees of *Q. cerris* and *Q. frainetto* could be due to their role as osmolytes or to impaired phloem functioning which prevents access to carbohydrate reserves (Sala et al. 2012).

However, these measured differences in NSC pools between declining and non-declining trees in *Q. pubescens* and *Q. frainetto* may have been also affected by

different water availability in summer across years. Indeed the tree-ring width data show that the differences between declining and non-declining trees arose much before the sampling date, especially in *Q. pubescens*. Of course, these prior (chronic) differences in growth may be due to several reasons (i.e. previous dieback episodes, disturbances, selective dead of trees with lowest growth rates, etc.), and may have differently predisposed trees to the 2010s droughts. However, non-declining and declining trees showed similar growth rates during dry periods (Fig. 2), whereas non-declining trees grew more than declining trees during wet years, except for *Q. frainetto* where declining trees displayed a higher BAI than non-declining trees around 1960s. These shifting responses indicate a reduced responsiveness to water shortage during that cool period which could explain the higher growth rate of declining trees. However, we cannot discard other potential drivers explaining the differences in growth rates including management, pests, fire or other climatic events (e.g., frosts, etc.). Such different growth responsiveness to drought and temperature variation can predispose trees to show decline in response to recent droughts and reconcile observations made at decadal to annual scales.

As previously observed (Colangelo et al. 2017b), declining trees were shorter than non-declining trees, regardless of species. This difference cannot be fully explained by changes in tree-to-tree competition intensity. Recently, declining trees also showed lower radial growth rates, thus reducing their sapwood cross-sectional area which would disproportionally affect their leaf and root production (Magnani et al. 2000). This could have magnified the disparity in scaling strategies between declining and non-declining trees leading to an irreversible drought-induced reduction in radial growth, hydraulic conductivity and carbon uptake. How successive and hotter droughts contribute to sharp

growth reductions and increased differences in vulnerability within a tree species is still unclear.

Tree-to-tree size variability could be connected to the observed differences in access to deep water pools since shorter declining trees could form shallower or less efficient root systems, thus relying more on superficial soil water than taller, deep-rooted, non-declining trees. Such allometric or scaling relationships (*cf*. Ledo et al. 2018) are understudied in the case of drought-induced dieback, and demand further research to assess how allocation patterns (i.e., root to shoot ratio) drive access to soil water and if these relationships are related to drought damage at the intra-specific level. Similar approaches have been carried out for interspecific comparisons (Olson et al. 2018). For example, large trees might form more extensive and deeper root systems or have a higher hydraulic capacitance (Bucci et al. 2005), and thus show a better capacity to tolerate drought stress. The assignment of such differences to adaptive variation in the responses to drought should also consider confounding factors as microsite differences (e.g., topography-mediated hydrologic refugia) or climate-driven changes in root to shoot ratios (e.g., Camarero et al. 2016, 2018).

The idea that declining trees may be less able to access to deep water pools than non-declining trees is supported by empirical studies. In an experimental setting where dry and warm conditions were induced, drought led to deeper water uptake in stressed trees relative to ambient, unstressed trees (Grossiord et al. 2017). Such shift in water uptake depth can be linked to a higher carbon allocation to deep roots under conditions of soil water depletion or elevated VPD during the dry summer (Bréda et al. 2006). This seasonal shift can disappear when precipitation increases and water sources from shallower soil layers become fully available (Voltas et al. 2015). In addition, the ability of roots to uptake increasing amounts of groundwater with extended and hotter droughts

is limited (Markewitz et al. 2010, Barbeta et al. 2015), and high soil temperature may restrain root activity and water and nutrients uptake in species with shallow roots or amplify soil hydrophobicity (Williams and Ehleringer 2000). Local factors like the differential access to deep water sources should be included in models to produce more realistic forecasts of forest dieback. Soil factors could explain why drought triggers dieback in sites where that was not an *a priori* expectation (Gazol et al. 2018).

Conclusions

We investigated tree-to-tree variability of radial growth, soil water uptake and NSC concentrations in three oak species showing drought-induced dieback. In peak summer, non-declining trees extracted deeper soil water than declining trees in *Q. cerris* and *Q. pubescens*, as indicated by significantly more depleted xylem water values, but this was not the case in *Q. frainetto*, a species which dominates in mesic sites. The evidence for deuterium fractionation taking place at the soil or plant level, however, prevented a proper quantification of the relevance of different water pools for tree transpiration. Declining trees showed lower height and radial-growth rate than non-declining trees. Sapwood starch concentrations were lower in declining trees in *Q. cerris* and *Q. pubescens*. To the extent of our knowledge, this is the first study showing how the differential access to deep water reservoirs influences drought-induced decay of individuals of a species population subjected to a dieback episode. Additional work should focus on the investigation of seasonal dynamics of water use, reserves and other physiological indicators (i.e., stable isotopes in dry matter) related to potential differences in water uptake capacity within the soil profile between healthy and declining trees.

Acknowledgements

This research was financially supported by the project OT4CLIMA (Italian Ministry of Education, Universities and Research – MIUR ARS01_00405) "Advanced EO Technologies for studying climate change impacts on the environment" and by the project "Alarm of forest mortality in Southern Italy" (Gorgoglione Administration, Basilicata Region, Italy). MC was supported by the PhD program from the University of Basilicata (Italy). JJC acknowledges funding by the project CGL2015-69186-C2-1-R project (Spanish Ministry of Economy). We acknowledge the E-OBS dataset from the EU-FP6 project UERRA (http://www.uerra.eu) and the data providers in the ECA&D project (https://www.ecad.eu).

References

Adams HD, Zeppel MJB, Anderegg WRL, Hartmann H, Landhäusser S, Tissue DT, Huxman TE, Hudson PJ, Franz TE, Allen CD, Anderegg LDL, Barron-Gafford GA, Beerling DJ, Breshears DD, Brodribb TJ, Bugmann H, Cobb RC, Collins AD, Dickman LT, Duan H, Ewers BE, Galiano L, Galvez DA, Garcia-Forner N, Gaylord ML, Germino MJ, Gessler A, Hacke UG, Hakamada R, Hector A, Jenkins MW, Kane JM, Kolb TE, Law DJ, Lewis JD, Limousin J-M, Love DM, Macalady AK, Martínez-Vilalta J, Mencuccini M, Mitchell PJ, Muss JD, O'Brien MJ, O'Grady AP, Pangle RE, Pinkard EA, Piper FI, Plaut JA, Pockman WT, Quirk J, Reinhardt K, Ripullone F, Ryan MG, Sala A, Sevanto S, Sperry JS, Vargas R, Vennetier M, Way DA, Xu C, Yepez EA, McDowell NG (2017) A multi-species synthesis of physiological mechanisms in drought-induced tree mortality. Nat Ecol Evol 1: 1285–1291.

Allen CD, Breshears DD, McDowell NG (2015) On underestimation of global vulnerability to tree mortality and forest die-off from hotter drought in the Anthropocene. Ecosphere 6: art129.

Anderegg WRL, Klein T, Bartlett M, Sack L, Pellegrini AF, Choat B, Jansen S (2016) Meta-analysis reveals that hydraulic traits explain cross-species patterns of drought-induced tree mortality across the globe. PNAS 113: 5024–5029.

Anderegg WRL, Konings AG, Trugman AT, Yu K, Bowling DR, Gabbitas R, Karp DS, Pacala S, Sperry JS, Sulman BN, Zenes N (2018) Hydraulic diversity of forests regulates ecosystem resilience during drought. Nature 561: 538–541.

Antunes C, Chozas S, West J, Zunzunegui M, Diaz Barradas MC, Vieira S, Máguas C (2018) Groundwater drawdown drives ecophysiological adjustments of woody vegetation in a semi-arid coastal ecosystem. Glob Ch Biol 24: 4894–4908.

Barbeta A, Mejía-Chang M, Ogaya R, Voltas J, Dawson TE, Peñuelas J (2015) The combined effects of a long-term experimental drought and an extreme drought on the use of plant-water sources in a Mediterranean forest. Glob Ch Biol 21: 1213–1225.

Barbeta A, Peñuelas J (2017) Relative contribution of groundwater to plant transpiration estimated with stable isotopes. Sci reports 7: 10580.

Barbeta A, Jones SP, Clavé L, Wingate L, Gimeno TE, Fréjaville B, Wohl S, Ogée J (2019) Unexplained hydrogen isotope offsets complicate the identification and quantification of tree water sources in a riparian forest. Hydrol Earth Syst Sci 23: 2129–2146.

Bréda N, Huc R, Granier A, Dreyer E (2006) Temperate forest trees and stands under severe drought: a review of ecophysiological responses, adaptation processes and long-term consequences. Ann For Sci 63: 625–644.

Bucci SJ, Goldstein G, Meinzer FC, Franco AC, Campanello P, Scholz FG (2005) Mechanisms contributing to seasonal homeostasis of minimum leaf water potential and predawn disequilibrium between soil and plant water potential in Neotropical savanna trees. Trees 19: 296–304.

Buysse J, Merckx R (1993) An improved colorimetric method to quantify sugar content of plant tissue. J Exp Bot 44: 1627–1629.

Cailleret M, Dakos V, Jansen S, Robert EMR, Aakala T, Amoroso MM, Antos JA, Bigler C, Bugmann H, Caccianaga M, Camarero JJ, Cherubini P, Coyea MR, Čufar K, Das AJ, Davi H, Gea-Izquierdo G, Gillner S, Haavik LJ, Hartmann H, Hereş A-M, Hultine KR, Janda P, Kane JM, Kharuk VI, Kitzberger T, Klein T, Levanic T, Linares J-C, Lombardi F, Mäkinen H, Mészáros I, Metsaranta JM, Oberhuber W, Papadopoulos A, Petritan AM, Rohner B, Sangüesa-Barreda G,

Smith JM, Stan AB, Stojanovic DB, Suarez M-L, Svoboda M, Trotsiuk V, Villalba R, Westwood AR, Wyckoff PH, Martínez-Vilalta J (2018) Early-warning signals of individual tree mortality based on annual radial growth. Front. Plant Sci., https://doi.org/10.3389/fpls.2018.01964

Camarero JJ, Gazol, A., Sangüesa-Barreda, G., Oliva, J. and Vicente-Serrano, S. M. 2015. To die or not to die: early-warning signals of dieback in response to a severe drought. J Ecol 103: 44–57.

Camarero JJ, Sangüesa-Barreda G, Vergarechea M (2016) Prior height, growth, and wood anatomy differently predispose to drought-induced dieback in two Mediterranean oak species. Ann For Sci 73: 341–351.

Camarero, JJ, Sánchez-Salguero, R, Sangüesa-Barreda G, Matías L (2018). Tree species from contrasting hydrological niches show divergent growth and water-use efficiency. Dendrochronologia 52: 87–95.

Castaño C, Lindahl BD, Alday JG, Hagenbo A, Martínez de Aragón J, Parladé J, Pera J, Bonet JA (2018) Soil microclimate changes affect soil fungal communities in aMediterranean pine forest. New Phytol 220: 1211–1221.

Chitra-Tarak R, Ruiz L, Dattaraja H S, Kumar MSM, Riotte J, Suresh HS, McMahon SM, Sukumar R (2018) The roots of the drought: hydrology and water uptake strategies mediate forest-wide demographic response to precipitation. J Ecol 106: 1495–1507.

Choat B, Brodribb TJ, Brodersen CR, Duursma RA, López R, Medlyn BE (2018) Triggers of tree mortality under drought. Nature 558: 531–539.

Colangelo M, Camarero JJ, Battipaglia G, Borghetti M, De Micco V, Gentilesca T, Ripullone F (2017°) A multi-proxy assessment of dieback causes in a Mediterranean oak species. Tree Physiol 37: 617-631

Colangelo M, Camarero JJ, Borghetti M, Gazol A, Ripullone F (2017b) Size matters a lot: drought-affected Italian oaks are smaller and show lower growth prior to tree death. Front Plant Sci 8: 135.

Colangelo M, Camarero JJ, Borghetti M, Gentilesca T, Oliva J, Ripullone F, Redondo MA (2018) Drought and *Phytophthora* are associated with the decline of oak species in southern Italy. Fron Plant Sci 9: 1595.

Cornes, R., G. van der Schrier, E.J.M. van den Besselaar, and P.D. Jones. (2018) An ensemble version of the E-OBS temperature and precipitation datasets. J. Geophys. Res. Atmos., 123: 9391-9409. doi:10.1029/2017JD028200.

Costa A, Pereira H, Madeira M (2010) Analysis of spatial patterns of oak decline in cork oak woodlands in Mediterranean conditions. Ann For Sci 67: 204.

Del Castillo J, Comas C, Voltas J, Ferrio JP (2016) Dynamics of competition over water in a mixed oak-pine Mediterranean forest: Spatio-temporal and physiological components. For Ecol Manage 382: 214–224.

Dubbert M, Werner C (2019) Water fluxes mediated by vegetation: emerging isotopic insights at the soil and atmosphere interfaces. New Phytol 221: 1754–1763.

Dubbert M, Caldeira MC, Dubbert D, Werner C (2019) A pool-weighted perspective on the two-water-worlds hypothesis. New Phytol 222: 1271–1283.

Duncan RP. 1989. An evaluation of errors in tree age estimates based on increment cores in Kahikatea *(Dacrycarpus* dacrydiodes). New Zealand Nat Sci 16: 31–37.

Ehleringer JR, Dawson TE (1992) Water uptake by plants: perspectives from stable isotope composition. Plant, Cell Env 15: 1073–1082.

Evaristo J, McDonnel JJ (2017) Prevalence and magnitude of groundwater use by vegetation: a global stable isotope meta-analysis. Sci. Reports 7:44110.

Gärtner H, Nievergelt D (2010) The core-microtome: a new tool for surface preparation on cores and time series analysis of varying cell parameters. Dendrochronologia 28: 85–92.

Gazol A, Camarero JJ, Jiménez JJ, Moret-Fernández D, López MV, Sangüesa-Barreda G, Igual JM. 2018. Beneath the canopy: linking drought-induced forest die off and changes in soil properties. For Ecol Manage 422: 294–302.

Gentilesca T, Camarero JJ, Colangelo M, Nolè A, Ripullone F (2017) Drought-induced oak decline in the western Mediterranean region: an overview on current evidences, mechanisms and management options to improve forest resilience. iForests 10: 796–806.

Greenwood S, Ruiz-Benito P, Martínez-Vilalta J, Lloret F, Kitzberger T, Allen CD, Kraft NJ (2017) Tree mortality across biomes is promoted by drought intensity, lower wood density and higher specific leaf area. Ecol Lett 20: 539–553.

Grossiord C, Sevanto S, Dawson TE, Adams HD, Collins AD, Dickman LT, Newman BD, Stockton EA, McDowell NG (2017) Warming combined with more extreme precipitation regimes modifies the water sources used by trees. New Phytol 213: 584–596.

Hasselquist NJ, Allen MF, Santiago LS (2010) Water relations of evergreen and drought-deciduous trees along a seasonally dry tropical forest chronosequence. Oecologia 164: 881–890.

Hentschel R, Rosner S, Kayler ZE, Andreassen K, Børja I, Solverg S, Tveito OE, Priescak E, Gessler A (2014) Norway spruce physiological and anatomical predisposition to dieback. For Ecol Manage 322: 27–36.

Holmes RL (1983) Computer-assisted quality control in tree-ring dating and measurement. Tree-Ring Res 43: 69–78.

Johnson DM, Domec JC, Carter Berry Z, Schwantes AM, McCulloh KA, Woodruff DR, Wayne Polley H, Wortemann R, Swenson JJ, Scott Mackay D, McDowell NG, Jackson RB (2018) Co-occurring woody species have diverse hydraulic strategies and mortality rates during an extreme drought. Plant Cell Env 41: 576–88.

Javaux M, Rothfuss Y, Vanderborght J, Vereecken H, Brüggemann N (2016) Isotopic composition of plant water sources. Nature 536 E1-E3.

Klein T (2014) The variability of stomatal sensitivity to leaf water potential across tree species indicates a continuum between isohydric and anisohydric behaviours. Funct Ecol 28: 1313–1320.

Körner C (2013) Growth controls photosynthesis – mostly. Nova Acta Leopoldina 114: 273–283.

Ledo A, Paul KI, Burslem DF, Ewel JJ, Barton C, Battaglia M, Brooksbank K, Carter J, Eid TH, England JR, Fitzgerald A, Jonson J, Mencuccini M, Montagu KD, Montero G, Mugasha WA, Pinkard E, Roxburgh S, Ryan CM, Ruiz-Peinado R, Sochacki S, Specht A, Wildy D, Wirth C, Zerihun A, Chave J (2018) Tree size and climatic water deficit control root to shoot ratio in individual trees globally. New Phytol 217: 8–11.

Lin G, Sternberg LSL (1993) Hydrogen isotopic fractionation by plant roots during water uptake in coastal wetland plants. In: Ehleringer J, Hall A, Farquhar G, eds. Stable isotopes and plant carbon-water relations. New York: Academic Press Inc., 497–510.

Liu H, Gleason SM, Hao G, Hua L, He P, Goldstein G, Ye G (2019) Hydraulic traits are coordinated with maximum plant height at the global scale. Sci. Adv. 5: eaav1332.

Magnani F, Mencuccini M, Grace J (2000) Age-related decline in stand productivity: the role of structural acclimation under hydraulic constraints. Plant Cell Env 23: 251–263.

Markewitz D, Devine S, Davidson EA, Brando P, Nepstad DC (2010) Soil moisture depletion under simulated drought in the Amazon: Impacts on deep root uptake. New Phytol 187: 592–607.

Martín-Gómez P, Barbeta A, Voltas J, Peñuelas J, Denis K, Palacio S, Dawson TE, Ferrio JP (2015) Isotope ratio infrared spectroscopy: a reliable tool for the investigation of plant-water sources? New Phytol 207: 914–927.

Martín-Gómez P, Serrano L, Ferrio JP (2017a) Short-term dynamics of evaporative enrichment of xylem water in woody stems: implications for ecohydrology. Tree Physiol 37: 511-522.

Martín-Gómez P, Aguilera M, Pemán J, Gil-Pelegrín E, Ferrio JP (2017b) Contrasting ecophysiological strategies related to drought: the case of a mixed stand of Scots pine (*Pinus sylvestris*) and a submediterranean oak (*Quercus subpyrenaica*). Tree Physiol 37: 1478–1492.

Martin-StPaul N, Delzon S, Cochard H (2017) Plant resistance to drought depends on timely stomatal closure. Ecol Lett 20: 1437–1447.

McDowell NG, Pockman WT, Allen CD, Breshears DD, Cobb N, Kolb T, Plaut J, Sperry JS, West A, Williams DG, Yepez EA (2008) Mechanisms of plant survival and mortality during drought: why do some plants survive while others succumb to drought? New Phytol 178: 719–739.

McDowell NG, Allen CD (2015) Darcy's law predicts widespread forest mortality under climate warming. Nat Clim Ch 5: 669–672.

McLaughlin BC, Ackerly DD, Klos PZ, Natali J, Dawson TE, Thompson SE (2017) Hydrologic refugia, plants, and climate change. Glob Ch Biol 23: 2941–2961.

Meinzer FC, Andrade JL, Goldstein G, Holbrook NM, Cavelier J, Wright SJ (1999) Partitioning of soil water among canopy trees in a seasonally dry tropical forest. Oecologia 121: 293–301.

Moreno-Gutierrez C, Dawson TE, Nicolas E, Querejeta JI (2012). Isotopes reveal contrasting water use strategies among coexisting plant species in a Mediterranean ecosystem. New Phytol 196: 489–496.

Muller B, Pantin F, Génard M, Turc O, Freixes S, Piques M, Gibon Y (2011) Water deficits uncouple growth from photosynthesis, increase C content, and modify the relationships between C and growth in sink organs. J Exp Bot 62: 1715–1729.

Nardini A, Lo Gullo MA, Salleo S (2011) Refilling embolized xylem conduits: is it a matter of phloem unloading? Plant Sci 180(4), 604-611.

Nardini A, Battistuzzo M, Savi T (2013) Shoot desiccation and hydraulic failure in temperate woody angiosperms during an extreme summer drought. New Phytol 200: 322–329.

Oerter EJ, Bowen GJ (2019) Spatio-temporal heterogeneity in soil water stable isotopic composition and its ecohydrologic implications in semi-arid ecosystems. Hydrol Process 33: 1724–1738.

Olson ME, Soriano D, Rosell JA, Anfodillo T, Donoghue MJ, Edwards EJ, León-Gómez C, Dawson T, Camarero JJ, Castorena M, Echeverría A, Espinosa CI, Fajardo A, Gazol A, Isnard S, Lima RS, Marcati CR, Méndez-Alonzo R (2018)

Plant height and hydraulic vulnerability to drought and cold. PNAS 115: 7551–7556.

Orlowski N, Breuer L, Angeli N, Boeckx P, Brumbt C, Cook CS, Dubbert M, Dyckmans J, Gallagher B, Gralher B, Herbstritt B, Hervé-Fernández P, Hissler C, Koeniger P, Legout A, Joan Macdonald C, Oyarzún C, Redelstein R, Seidler C, Siegwolf R, Stumpp C, Thomsen S, Weiler M, Werner C, McDonnell JJ (2018) Inter-laboratory comparison of cryogenic water extraction systems for stable isotope analysis of soil water. Hydrol Earth Syst Sci 22: 3619–3637.

Otieno DO, Kurz-Besson C, Liu J, Schmidt MWT, Vale-Lobo d, David TS, Siegwolf R, Pereira JS, Tenhunen JD (2006) Seasonal variations in soil and plant water status in a *Quercus suber* L. stand: roots as determinants of tree productivity and survival in the Mediterranean-type ecosystem. Plant Soil 283: 119–135

Dinamic, structured heterogeneity of water isotopes inside hillslopes (2015) Oshun J, Dietrich WE, Dawson TE, Fung I Water Resource Res 52(1): 4840–4847.

Padilla FM, Pugnaire FI (2007) Rooting depth and soil moisture control Mediterranean woody seedling survival during drought. Funct Ecol 21: 489–495.

Palacio S, Azorin J, Montserrat-Martì G, Ferrio JP (2014) The crystallization water of gypsum rocks is a relevant water source for plants. Nature Commun 5: 4660.

Paternoster M, Liotta M, Favara R (2008) Stable isotope ratios in meteoric recharge and groundwater at Mt. Vulture volcano, southern Italy. J Hydrol 348: 87–97.

Pfautsch S, Renard J, Tioelker MG, Salih A (2015) Phloem as Capacitor: Radial Transfer of Water into Xylem of Tree Stems Occurs via Symplastic Transport in Ray Parenchyma. Plant Physiol 167(3): 963–971.

Pinheiro HA, DaMatta FM, Chaves AR, Loureiro ME, Ducatti C (2005) Drought tolerance is associated with rooting depth and stomatal control of water use in clones of *Coffea canephora*. Ann Bot 96: 101-108.

Pivovaroff AL, Pasquini SC, De Guzman ME, Alstad KP, Stemke JS, Santiago LS (2016) Multiple strategies for drought survival among woody plant species. Funct Ecol 30: 517–526.

Poca M, Coomans O, Urcelay C, Zeballos SR, Bodé S, Boecks P (2019) Isotope fractionation during root water uptake by *Acacia caven* is enhanced by arbuscular mycorrhizas. Plant Soil 441: 485–497.

Rempe DM and Dietrich WE (2018) Direct observations of rock moisture, a hidden component of the hydrologic cycle. Proc Natl Acad Sci 115(11): 2664–2669.

Sala A, Woodruff DR, Meinzer FC (2012) Carbon dynamics in trees: feast or famine? Tree Physiol 32: 764–775.

San-Miguel-Ayanz J, de Rigo D, Caudullo G, Houston Durrant T, Mauri A (Eds.) (2016) European Atlas of Forest Tree Species. European Union, Luxembourg.

Sánchez-Salguero R, Camarero JJ, Carrer M, Gutiérrez E, Alla AQ, Andreu-Hayles L, Hevia A, Koutavas A, Martínez-Sancho E, Nola P, Papadopoulos A, Pasho E, Toromani E, Carreira JA, Linares JC (2017) Climate extremes and predicted warming threaten Mediterranean Holocene fir forests refugia. PNAS 14: E10142–E10150.

SAS (2015) SAS Institute Inc. SAS/STAT®14.1 User's Guide. Cary, NC, USA.

Shestakova TA, Aguilera M, Ferrio JP, Gutiérrez E, Voltas J (2014) Unravelling spatiotemporal tree-ring signals in Mediterranean oaks: a variance–covariance modelling approach of carbon and oxygen isotope ratios. Tree Physiol 34: 819–838.

Tardieu F, Granier C, Muller B (2011) Water deficit and growth. Co-ordinating processes without an orchestrator? Curr Opinion in Plant Biol 14: 283–289.

Tognetti R, Longobucco A, Raschi A (1998) Vulnerability of xylem to embolism in relation to plant hydraulic resistance in *Quercus pubescens* and *Quercus ilex* co-occurring in a Mediterranean coppice in central Italy. New Phytol 139: 437–447.

Vargas AI, Schaffer B, Yuhong L, Sternberg LSL (2017) Testing plant use of mobile vs immobile soil water sources using stable isotope experiments. New Phytol 215: 582–594.

Voltas J, Camarero JJ, Carulla D, Aguilera M, Ortiz A, Ferrio JP (2013) A retrospective, dual-isotope approach reveals individual predispositions to winter-drought induced tree dieback in the southernmost distribution limit of Scots pine. Plant Cell Environ 36: 1435–1448.

Voltas J, Lucabaugh D, Chambel MR, Ferrio JP (2015) Intraspecific variation in the use of water sources by the circum-Mediterranean conifer *Pinus halepensis*. New Phytol 208: 1031–1041.

Wells N, Goddard S and Hayes MJ (2004) A self-calibrating Palmer Drought Severity Index. J Clim 17: 2335-2351.

Williams DG, Ehleringer JR (2000) Intra- and interspecific variation for summer precipitation use in pinyon–juniper woodlands. Ecol Monogr 70: 517–537.

Zhao L, Wang L, Cernusak LA, Liu X, Xiao H, Zhou M, Zhang S (2016) Significant difference in Hydrogen isotope composition between xylem and tissue water in *Populus euphratica*. Plant Cell Environ 39: 1848–1857.

Tables

Table 1. Main structural characteristics of the declining (D) and non-declining (ND) trees of the three study oak species (*Q. pubescens, Q. cerris*, and *Q. frainetto*). Values are means ± SE. Different letters indicate significant differences at the 0.05 level based on Mann-Whitney tests.

Tree species	Vigor class	Density (trees ha^{-1})	Diameter at 1.3 m (cm)	Height (m)	Age at 1.3 m (years)
Quercus pubescens	D	83 ± 6a	24.7 ± 0.7a	8.6 ± 0.3a	110 ± 3a
	ND	100 ± 11a	25.8 ± 0.9a	11.3 ± 0.3b	115 ± 4a
Quercus cerris	D	262 ± 16b	29.3 ± 0.8a	12.2 ± 0.4a	107 ± 2a
	ND	148 ± 13a	32.0 ± 0.9a	15.0 ± 0.6b	102 ± 4a
Quercus frainetto	D	244 ± 14b	29.9 ± 1.2a	10.2 ± 0.3a	132 ± 4a
	ND	104 ± 12a	31.9 ± 1.4a	13.5 ± 0.5b	140 ± 5a

Table 2. Comparisons of radial-growth rates (BAI, basal area increment) between coexisting non-declining (ND) and declining (D) trees of the three study oak species. Values are means ± SE. Different letters among BAI averages indicate significant differences at the 0.05 level based on Mann-Whitney tests. The lowermost row shows periods when ND trees grew significantly ($p < 0.05$) more than D trees according to Wilcoxon rank-sum tests.

	Quercus cerris	*Quercus frainetto*	*Quercus pubescens*
Mean BAI ND trees 1991- 2016 (mm^2)	884.26 ± 63.86b	655.99 ± 26.82b	448.51 ± 17.48b
Mean BAI D trees 1991- 2016 (mm^2)	408.70 ± 24.77a	424.58 ± 26.01a	259.56 ± 11.32a
Periods with BAI of ND trees > D trees	1953-1987, 1991–2016	1933-1947, 2002–2016	1937-1944, 1953–1961, 1984–1987, 1991–2016

Table 3. Sapwood concentrations of non-structural carbohydrates (NSC) shown as soluble sugars (SS), starch and total NSC and measured in declining (D) and non-declining (ND) oak trees. Values are means ± SE. Different letters indicate significant differences ($p < 0.05$; Mann-Whitney tests) between vigor classes within each species.

Species	Tree type	SS (%)	Starch (%)	NSC (%)
Quercus pubescens	D	2.28 ± 0.16a	1.82 ± 0.13a	4.10 ± 0.24a
	ND	2.22 ± 0.21a	3.24 ± 0.35b	5.46 ± 0.43b
Quercus cerris	D	2.03 ± 0.12b	2.05 ± 0.23a	4.08 ± 0.27a
	ND	1.62 ± 0.11a	2.89 ± 0.34b	4.51 ± 0.29a
Quercus frainetto	D	2.14 ± 0.12b	3.26 ± 0.28a	5.40 ± 0.42b
	ND	1.48 ± 0.13a	2.93 ± 0.33a	4.41 ± 0.44a

Table 4. *F*-values of three-way ANOVAs calculated on xylem water isotope values (δ^2H, $\delta^{18}O$) measured in samples from declining and non-declining individuals (*Tree type*) of three oak species (*Species*). Branch position (*Position*) was also considered as an effect in the analyses. The probability of the *F* values is shown between parentheses.

Effect	δ^2H (‰)	$\delta^{18}O$ (‰)	SW-excess (‰)
Species	94.47 (< 0.001)	90.07 (< 0.001)	41.58 (<0.001)
Tree Type	0.00 (0.961)	7.28 (0.007)	2.61 (0.108)
Branch Position	0.34 (0.563)	0.23 (0.633)	0.10 (0.751)
Species × Type	4.73 (0.010)	6.28 (0.002)	0.90 (0.409)
Species × Position	0.35 (0.702)	0.29 (0.748)	0.22 (0.799)
Type × Position	0.21 (0.651)	0.05 (0.812)	0.50 (0.480)
Species × Type × Position	0.94 (0.395)	0.36 (0.659)	0.85 (0.429)

Figure legends

Figure 1. Mean Palmer Drought Severity Index (PDSI) of the summer season (June to August; black bars, unitless) and mean annual temperature (red line) for the period of 1950-2017. Negative and positive PDSI values indicate dry and wet conditions, respectively.

Figure 2. Mean series of radial growth (expressed as basal area increment) from 1900 to 2016 considering declining and non-declining trees of the three study oak species: (a) *Quercus cerris*, (b) *Quercus frainetto*, and (c) *Quercus pubescens*.

Figure 3. Box-plots at the species level of (a) gravimetric soil water content (GWC) depending on the sampled soil layer (top or bottom soil) and (b) SW-excess depending on tree type (declining or non-declining). Box size represents the interquartile range, the black line is the median, the whiskers indicate variability outside the upper and lower quartiles, and individual points are outliers. In the case of GWC, only the interquartile range is depicted due to low sampling size.

Figure 4. Mean values (±SE) of (a) oxygen ($\delta^{18}O$) and (b) hydrogen ($\delta^{2}H$) isotopic compositions of xylem water in declining (D) and non-declining (ND) trees of the three studied oak species.

Figure 5. *Top panels*. Water isotope values ($\delta^{18}O$ and $\delta^{2}H$) of individual soil samples of oak stands (a, *Quercus pubescens*; b, *Quercus cerris*; c, *Quercus frainetto*). Soil water isotopes are included in the panels as follows: 0-15 cm depth (dark brown circles), 15-

30 cm (sandy brown circles), and source-based (springs, wells) groundwater estimates (blue circles). The slope (*b*) and goodness-of-fit (R^2) of the isotopic soil water line at the stand level (solid black lines) are included in the panels. *Bottom panels*. Xylem water isotope values ($\delta^{18}O$ and $\delta^{2}H$) of non-declining (green, filled circles) and declining trees (empty circles) of oak species (d, *Quercus pubescens*; e, *Quercus cerris*; f, *Quercus frainetto*). Mean values of soil water isotopes are included in the panels as follows (means ± SE): 0-15 cm depth (dark brown circles), 15-30 cm (sandy brown circles), source-based groundwater estimates (blue circles), and precipitation-based groundwater estimates (black squares). The solid black, dashed blue and dotted black lines indicate the isotopic soil water line, the local meteoric water line (LMWL), and the global meteoric water line (GMWL) respectively. The LMWL shows the linear variation of the isotopic composition of precipitation events in the study area.

947 **Figures**

948

949

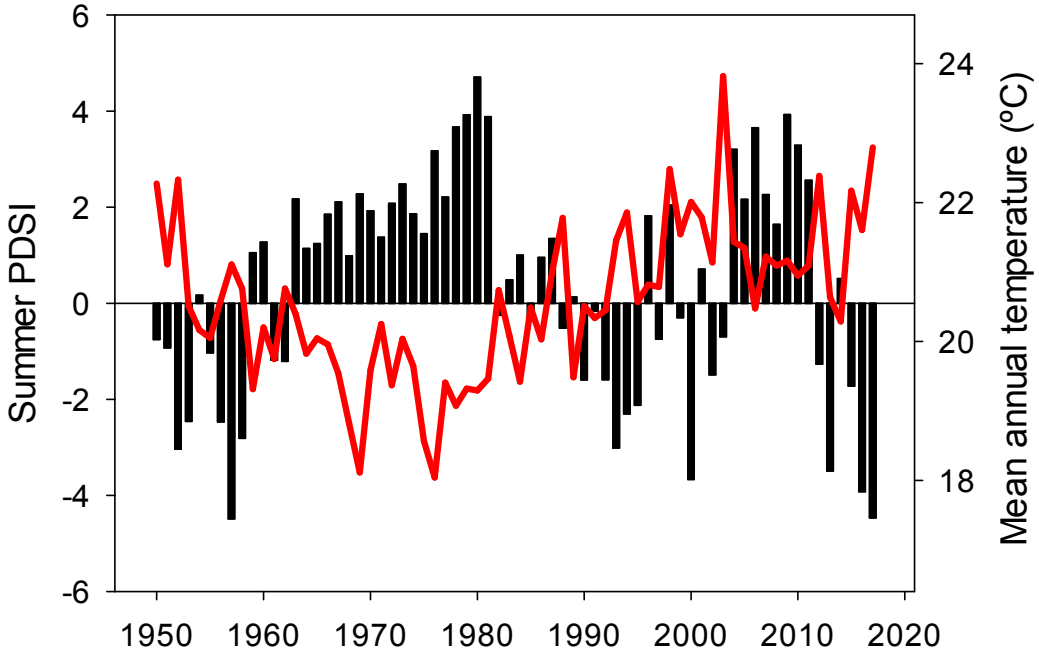

950

951

952 **Figure 1**

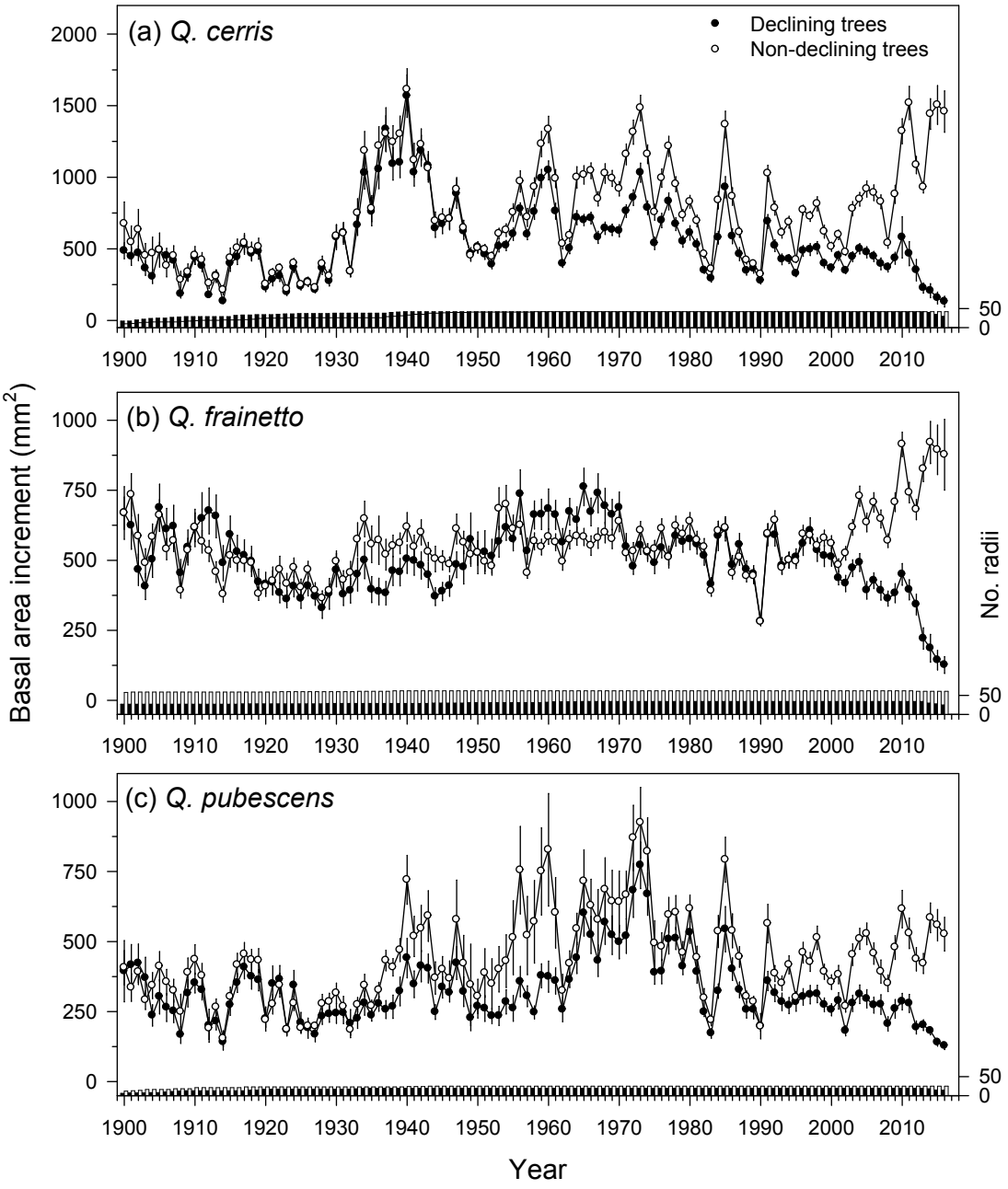

953

954

955 **Figure 2**

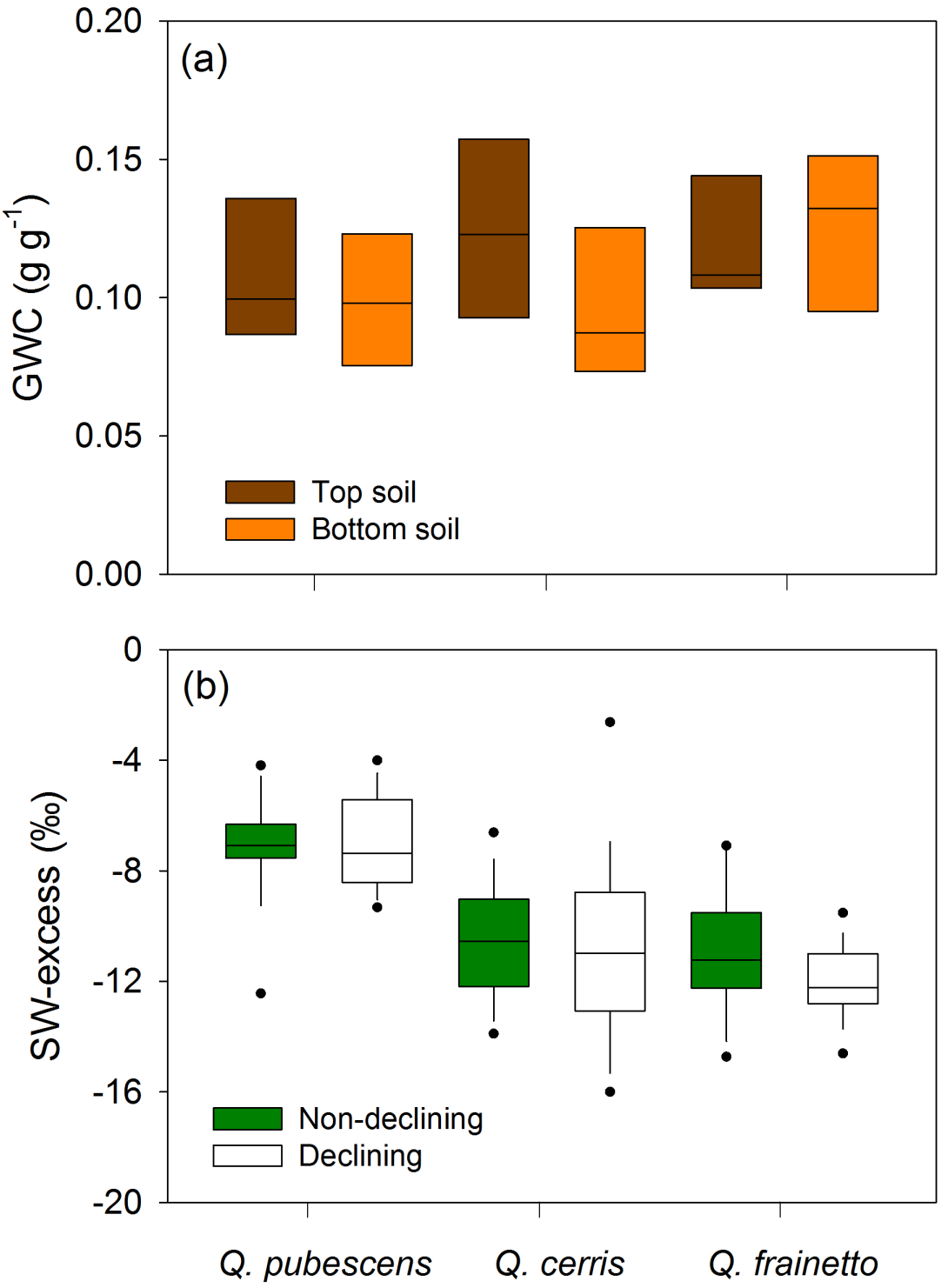

956

957 **Figure 3**

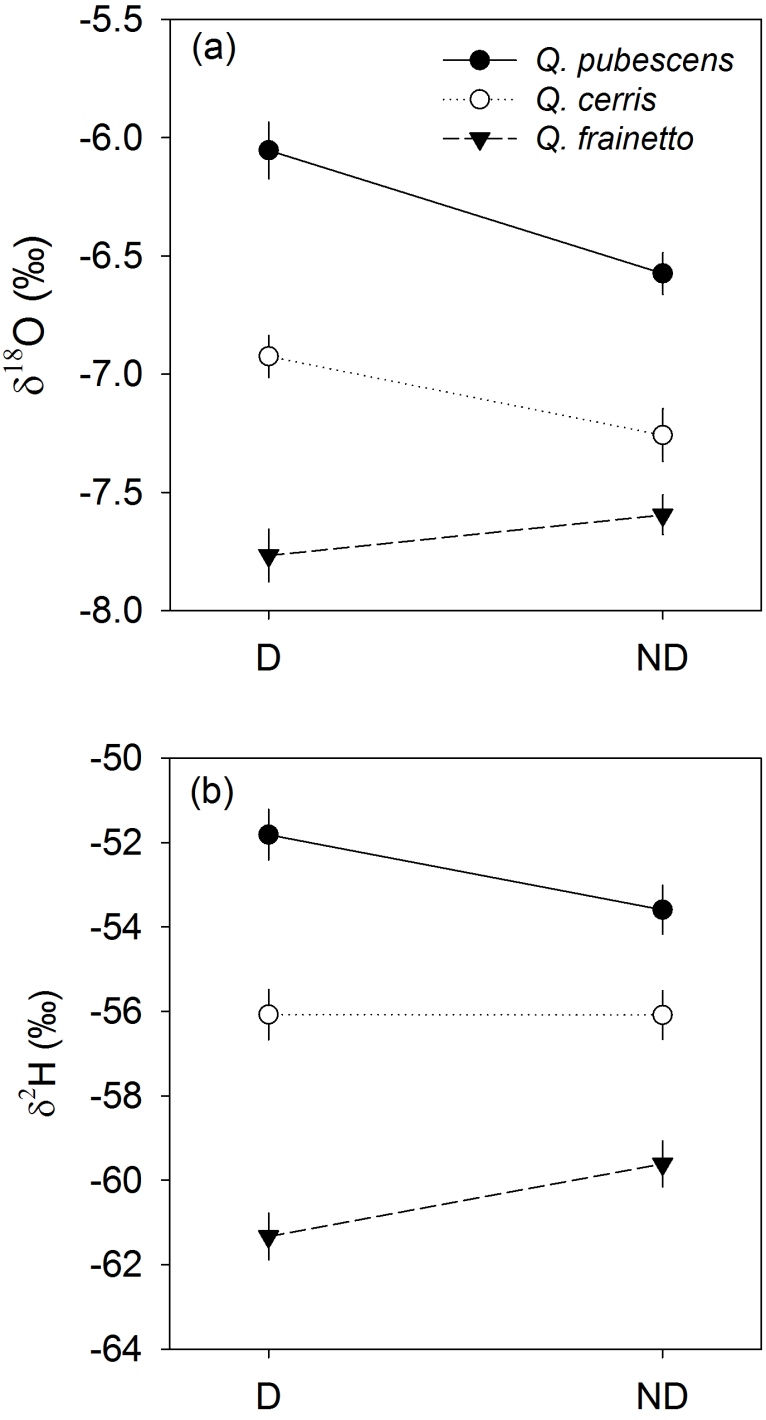
(a)
Q. pubescens
Q. cerris
Q. frainetto
-5.5
-6.0
-6.5
-7.0
-7.5
-8.0
δ18O (‰)
D
ND
(b)
-50
-52
-54
-56
-58
-60
-62
-64
δ2H (‰)
D
ND

Figure 4

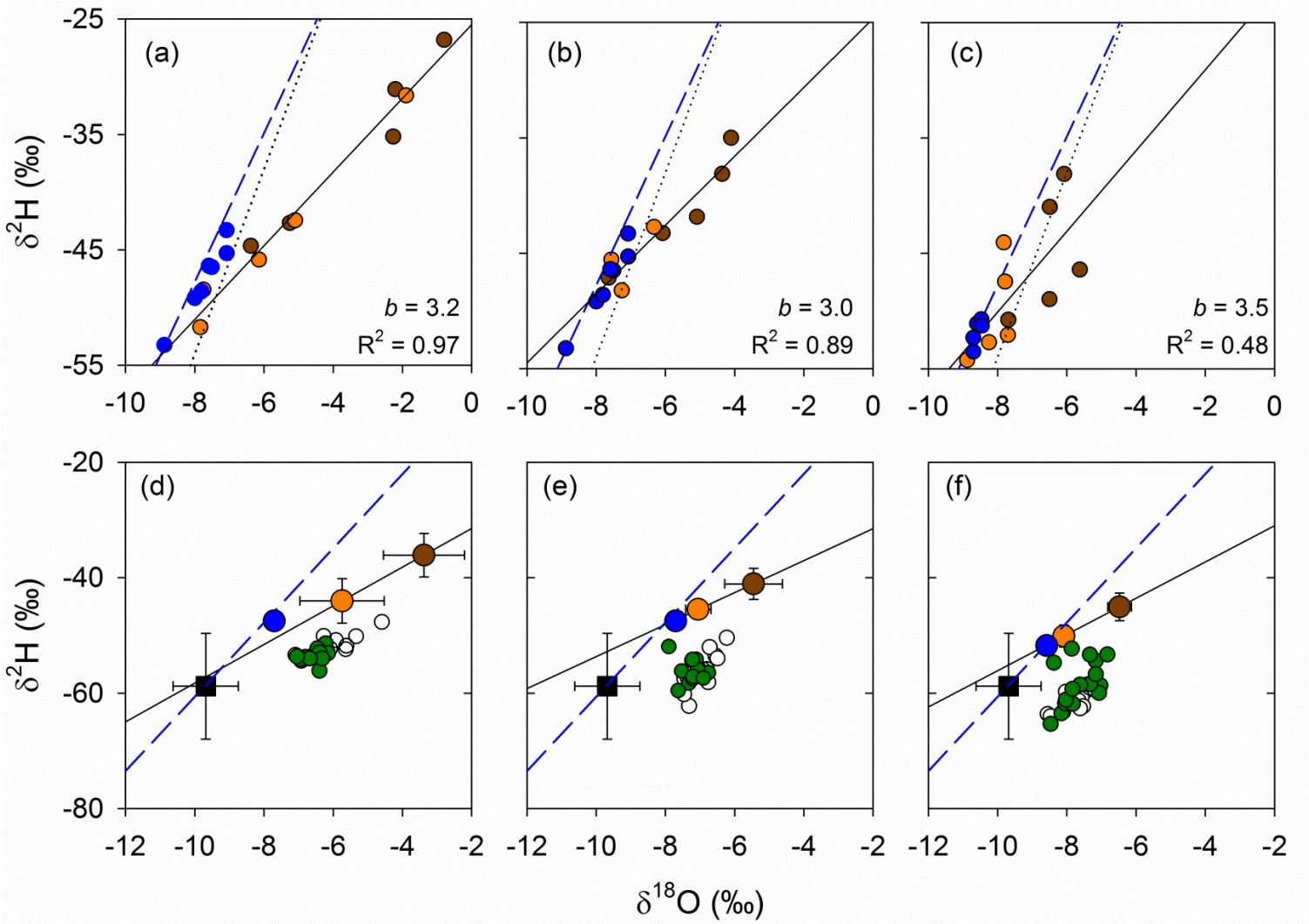
(a)
(b)
(c)
(d)
(e)
(f)
b = 3.2
R2 = 0.97
b = 3.0
R2 = 0.89
b = 3.5
R2 = 0.48
δ2H (‰)
δ18O (‰)
-25
-35
-45
-55
-20
-40
-60
-80
-10
-8
-6
-4
-2
0
-12

Figure 5